Loess genesis and worldwide distribution

Li, Yanrong; Shi, Wenhui; Aydin, Adnan et al.

(2020)

DOI (TUprints): https://doi.org/10.25534/tuprints-00017375

Publication type: Article

Division: 13 Department of Civil and Environmental Engineering Sciences

Original source: https://tuprints.ulb.tu-darmstadt.de/17375

Earth-Science Reviews 201 (2020) 102947

Contents lists available at ScienceDirect

Earth-Science Reviews

journal homepage: www.elsevier.com/locate/earscirev

Loess genesis and worldwide distribution

Yanrong Li[a,*], Wenhui Shi[a], Adnan Aydin[b], Mary Antonette Beroya-Eitner[c], Guohong Gao[a]

[a] Department of Earth Sciences and Engineering, Taiyuan University of Technology, Taiyuan 030024, China
[b] Department of Geology and Geological Engineering, University of Mississippi, Oxford, USA
[c] EarthThink Inc., San Juan, Metro Manila, Philippines

ARTICLE INFO

Keywords:
Loess
Genesis
Spatial distribution
Thickness
Coverage

ABSTRACT

Loess formation generally involves the four main stages of production, deflation, transportation, and deposition of loess particles. Traditionally, loesses are classified as glacial, desert, or other types based only on source area characteristics without taking into account provenance and transportation. Research on loess genesis is often local with only a few attempts at systematically overviewing worldwide loess distribution. Both the local and few global studies lack information on the variability in loess thickness, continuity, and areal extent. This review integrates a large body of information on loess source areas and transportation pathways and the existence of desert transition zones. Three modes of loess genesis, (1) continental glacier provenance-river transport, (2) mountain provenance-river transport, and (3) mountain provenance-river transport-desert transition, were identified. Global distribution maps of provenance and transport pathways of major loess areas and their different genesis modes were meticulously prepared. Maps showing the spatial distribution, thickness, and continuity of loess deposits were also composed and the sizes of loess-covered areas of each continent were re-estimated. The main features related to the distribution of the loess deposits on each continent are summarized for different regions or as a whole depending on the coverage of the source maps and references.

1. Introduction

Loess is a loose aeolian deposit of yellowish silt-sized dust mostly formed during the Quaternary period. Generally, it has a homogenous and porous structure and consists primarily of quartz and felspar particles.

Ancient Chinese scholars linked the formation of loess to wind-blown dust 2000 years ago. The Eastern Han Dynasty historian Fu Wuji wrote "yellow dust rained from sky" in 78 BCE in his book *Commentaries on Antiquity and Today*. Ban Gu, also an Eastern Han Dynasty historian, recorded "raining yellow dust lands on the ground all day long" in 32 BCE (Liu, 1985; Liu et al., 2001). Since Leonhard named loess in Heidelberg in 1824 and Charles Lyell (1833) made loess popular globally through his work *Principles of Geology* (Smalley et al., 2001), many theories pertaining to loess genesis, including Neptunian (e.g., alluvial, diluvial, and aqueoglacial deposit theories), residual slope products, pedogenesis (i.e., eluvial), and polygenesis theories (Li and Sun, 2005; Lei, 2014), have been put forth. Virlet D'Aoust (1857) observed that cyclones deflating alluvial deposits in the Central Mexican Plateau to the uplands formed loess-like deposits, marking the beginning of the modern aeolian theory (Liu et al., 1985; Li and Sun, 2005). Richthofen (1877) investigated the loess in China, compared it to the loess in his hometown adjacent to the Rhine River, and concluded that wind and water brought in weathering products from the surrounding hillsides that filled basins and formed loess. Subsequently, the aeolian theory was gradually accepted with ongoing modifications (Smalley et al., 2001).

Loess formation generally involves the four stages of production, deflation, transportation, and deposition of particles (Smalley, 1966; Wright, 2001; Muhs et al., 2014). For the first time, loess was linked to glaciers when Tutkovskii (1899) proposed that loess accumulated due to silty dust transported from glacial regions by foehn (down-slope winds) (Smalley et al., 2001). Obruchev (1911) believed loess in northern China was blown from the deserts in northwest China and first proposed the concept of "desert" loess. Obruchev (1933, 1958) called the Chinese loess blown from deserts "warm" loess and the central and western European loess blown from moraine areas "cold" loess (Liu et al., 1985; Smalley et al., 2001). Smalley (1966) and Smalley and Vita-Finzi (1968) further differentiated between typical glacial- and desert-originating loess, respectively. Pye (1987) summarized the origins of loess in Europe, China, and Central Asia and pointed out the vagueness of prior literature concerning the provenance and transportation history of loess deposits. Based on geomorphological and meteorological constraints, Liu et al. (1985) inferred that Chinese loess is

* Corresponding author.
E-mail address: li.dennis@hotmail.com (Y. Li).

https://doi.org/10.1016/j.earscirev.2019.102947
Received 7 March 2019; Received in revised form 28 April 2019; Accepted 1 September 2019
Available online 05 September 2019

mainly blown from the gobi (stony deserts) and sandy deserts in Northwest and North China. Sun (2002a,b) used geochemical methods to confirm that the loess in the Chinese Loess Plateau formed from materials derived from the Qilian and Gobi-Altay Mountains and transported via rivers and winds. Wright (2001) compared loess formation pathways in several typical loess areas.

The source areas and river transport processes for different areas were summarized by Bettis et al. (Bettis et al., 2003, North America), Chlachula (2003, Siberia), Eden and Hammond (2003, New Zealand), Dodonov (2007, Central Asia), and Zárate (2007, South America). Smalley et al. (2009) suggested that the main source of the loess particles in Central and Western Europe was the Alps Mountains, whereas the main source of the extensive loess deposits in eastern Europe was the Quaternary continental glacial region to the north with the materials transported by a number of rivers in meltwater and then wind. Smalley et al. (2009) focused on the key role of river transport in the formation of loesses, while Muhs (2007, 2013b) provided an overview of the formation patterns of several major desert and glacial loess regions worldwide.

Literature reviews in recent decades have gradually improved the descriptions and mapping of loess distribution around the world. For North American loess, 1:2,500,000 aeolian deposit maps have been drawn by the National Research Council Committee for the Study of Aeolian Deposits Division of Geology and Geography (NRCCED, 1952). Based on extensive field investigations, Liu (1965) prepared a map of the Chinese loess distribution that was supplemented with a detailed descriptive book. Eden and Hammond (2003) drew a sketch map of loesses in New Zealand based on the existing literature. Zárate (2007) summarized different references to create a sketch map of the loess distribution in South America. Haase et al. (2007) summarized references from various countries and drew a map of European loesses with a brief descriptive summary. Crouvi et al. (2010) compiled the sketch maps of loess distribution in Africa and the Arabian Peninsula. Some authors also provided a brief overview of the global loess distribution. For instance, Pye (1987) and Li and Sun (2005) presented simple schematic maps and descriptions of the global loess distribution that reflected the lack of detail in the literature at the time. Muhs (2013b) and Muhs et al. (2014) redrew the loess distribution maps for each continent, also showing the extent of certain continental ice sheets and providing brief descriptions.

At present, the literature on the origin of loesses consists of local or type-specific studies and lacks global overview, particularly holistic analyses and consideration of transport processes. The currently available global distribution maps and local studies on which they are based do not contain consistent and uniform information on loess thickness, continuity, and areal extent.

In this paper, the features of source areas and transport paths were critically reviewed and three loess genesis modes were proposed to classify and describe major loess regions around the world. A series of global loess distribution maps, which include information on loess genesis mode, transport path, thickness, and continuity, were generated and the areal extents of loesses were re-estimated from a systematic summary of the literature.

2. Loess genesis

To determine loess provenance or origin, pioneering researchers divided loess deposits into two types according to their source area, i.e., glacial or cold loess and desert or warm (hot) loess (e.g., Smalley, 1966; Smalley and Vita-Finzi, 1968; Muhs and Bettis, 2003; Muhs, 2007, 2013a,b; Muhs et al., 2014). The glacial loesses originate from mountain glaciers or continental glacier regions and are mainly the result of grinding of the glacier body against bedrock (Smalley, 1966; Muhs et al., 2014). Smalley and Derbyshire (1990) referred to loesses in the Central United States and Eastern Europe as ice-sheet loess because of their continental glacier origin. The loess material was transported away from the ice sheet in meltwater and these outwash deposits then became the primary source for the loess.

For a long time, the mechanism underlying the production of source material for desert loesses was not well understood. Originally, silt dust in some loess areas was observed to come from deserts traveling in an upwind direction, which is why deserts are considered the source areas (Smalley and Vita-Finzi, 1968; Liu et al., 1985; Crouvi et al., 2010). Subsequent research showed that the actual source areas were the surrounding mountains or uplands providing a continuous supply of particles to the deserts via fluvial transport, e.g., Tianshan Mountains in northwestern China (Smalley and Krinsley, 1978; Wright, 2001; Sun, 2002a; Muhs, 2013b; Smalley et al., 2014).

The term "mountain loess" first appeared in a discussion by Smalley (1978) on New Zealand loess (Smalley, 2008). Smalley and Derbyshire (1990) specifically used this term to explain the source of large deposits of desert loess and replace the term "desert loess". However, some glacial loesses are also derived from mountainous areas.

In South America, Iceland, Alaska, and New Zealand, volcanic ash is one of the major sources of loesses (Muhs et al., 2014). Therefore, the term "non-glacial" loess is used to differentiate between loess deposits made from silt-sized materials derived by non-glacial mechanisms, including weathering due to frost, salinization, insolation, and biological processes, fluvial comminution, aeolian abrasion, and volcanism (Pye, 1995; Wright, 2001; Smith et al., 2002; Muhs and Bettis, 2003; Crouvi et al., 2010).

Muhs et al. (2014) pointed out that the loess in certain areas has multiple origins, both glacial and non-glacial, and transport forms. Therefore, a specific loess area may not be accurately described by any of the proposed terms that only consider the characteristics of the source area. These classifications (e.g., glacial, desert, ice-sheet, mountain, and non-glacial) seem simple and intuitive, and the elements in each group either overlap to some degree or fail to cover all types of loesses.

After the production of the original transportable particles in a source area, they reach the loess accumulation areas by fluvial and aeolian relay transportation and transformation. Wind is the dominant mode of transport (Liu et al., 1985; Pye, 1995), but the important role of river transport prior to wind transport was recognized recently because many loess areas are located along rivers (Smalley, 1995; Smith et al., 2002). For most global loess areas, river transport also plays a key role in determining the migration direction and geographical distribution of particulate materials and sites of loess accumulation (Smalley, 1995; Smalley et al., 2009). Fluvial transport is enabled by various forms of surface runoff, including mountain streams with high potential energy fed by precipitation or glacial meltwater, mountain flash floods in arid and semi-arid regions induced by short-term heavy precipitation, and rivers into which mountain runoff converges. Fluvial transport is capable of carrying large amounts of particles from the source areas in the upper (higher) regions to outwash areas, alluvial-proluvial fans, alluvial plains (braided river areas and floodplains), and semi-enclosed desert basins in the middle and lower reaches (Smalley, 1995; Smith et al., 2002; Porter, 2007; Smalley et al., 2009). Sediments from which the clay mineral (cohesive) particles have been washed away are more vulnerable to deflation of exposed surfaces (Pye, 1995; Wright, 2001).

The subsequent aeolian processes, which are usually dominated by winter and spring winds (Liu et al., 2001), involve deflation of weakly vegetated surfaces in arid and semi-arid areas, such as mountainous regions, proluvial fans, floodplains, alluvial plains, and deserts, entrainment of particles into the air, transport for a certain distance, and finally deposition of loess-sized particles. Presently, dust storms are a direct example of this process (Pye, 1995; Dodonov, 2007; Muhs, 2013a). Aeolian transport and deposition provide loesses with special properties that render them different from soil and rock masses (Smalley et al., 2009). Source materials often reach the final loess accumulation zone through more than one stage of fluvial and/or wind transport (Pye, 1987).

Table 1
Summary of global loess provenance and transportation.

Loess genesis mode	Continent	Region	Source area (Highest elevation, m)	River & maximum transportation distance (km)	Main deflation area	Wind & maximum transportation distance (km)	References
CR Mode	Europe	Ukraine, Belarus, Moldova and southwestern Russia	Fennoscandian ice-sheet (primary source area); East piedmont of Carpathians (secondary); Uplands in eastern Europe (secondary) (347)	Dnepr, ~900; Don, ~700; and Volga, ~1000	Margin of continental glacier; Alluvial plains	Westerlies, 250	Jefferson et al., 2003a; Muhs, 2007; Smalley et al., 2009; Rousseau et al., 2007; Schaetzl et al., 2018a
	North America	Central United States	Laurentide ice-sheet (primary); East piedmont of Rockies (secondary) (4399)	Missouri, ~1000; Mississippi, ~1000; and their tributaries	Margin of continental glacier, Valleys & Alluvial plains	Paleowinds from west or northwest, 300	Grimley, 2000; Muhs and Bettis, 2003; Roberts and Muhs, 2007; Muhs, 2007; Smalley et al., 2009
MR Mode	North America	Western United States	Rocky Mountains (4399)	Missoula Lake floods & Columbia River, ~400; Snake, ~350; and San Juan, ~200	River valley; Alluvial plains	Westerly or northwesterly winds, 100	Bettis et al., 2003; Busacca et al., 2003; Roberts and Muhs, 2007
		Alaska	Alaska Range (6914); Brooks Range (2816)	Tanana, ~300; Yukon, ~900; and Colville, ~200	River valley; Alluvial plains	Northeast & other winds, 200	Péwé, 1975; Busacca et al., 2003; Roberts and Muhs, 2007; Muhs et al., 2018
	South America	Gran Chaco & Pampa Ondulada (Argentina), Bolivia, Paraguay and Uruguay	Chilean Altiplano (Western Andes); Andes Cordillera (6960); Sierras Pampeanas (6250); Volcanoes in Puna plateau	Pilcomayo, ~800; Bermejo, ~700; Paraguay, ~200; and Paraná, ~800	Alluvial plains; Alluvial fans	Northerly wind (Chaco), 200; Westerly and southwesterly winds (Pampas), 200	Smalley, 1995; Iriondo, 1997; Sayago et al., 2001; Zárate, 2003; Zárate, 2007; Muhs et al., 2014
	Europe	France	Massif Central (1885) (primary); Western Alps Piedmont (primary); Fennoscandian ice-sheet (secondary)	Somme, Seine, Loire, Garonne, and Rhone, 150–300	Sandurs; Dried-out shelves; Alluvial plains	Westerlies & local winds, 200	Koster, 1988; Coudé-Gaussen, 1990; Lebret and Lautridou, 1991; Rousseau et al., 2007; Antoine et al., 2009; Smalley et al., 2009; Lehmkuhl et al., 2016
		Belgium	Alps Mountains (primary) (4810); Fennoscandian ice-sheet (secondary)	Meuse, ~200; and proto-Rhine, ~500	Dried-out shelves; Alluvial plains	Westerlies & local winds, unknown	Koster, 1988; Lebret and Lautridou, 1991; Hill, 2005; Rousseau et al., 2007; Antoine et al., 2009; Smalley et al., 2009
		Britain	Alps Mountains (primary) (4810); Fennoscandian ice-sheet (secondary)	Thames, ~100; and proto-Rhine, ~600	Dried-out shelves; Estuary regions	Westerlies & local winds, 100	Jefferson et al., 2003b; Hill, 2005; Smalley et al., 2009; Antoine et al., 2009
		Germany	Alps Mountains (4810); Sudetes Mountains	Rhine, ~300; Great Odra Valley, ~600; Elbe, ~200; and Danube	River valley; Alluvial plains; Dried-out shelves; Outwash	Westerlies & local winds, 150	Antoine et al., 2009; Smalley et al., 2009; Badura et al., 2013; Lehmkuhl et al., 2016
		Poland	Carpathian Mountains (2655); Sudetes Mountains (1602)	Great Odra Valley, ~300; and Vistula (Wisla), ~150	River valley; Alluvial plains	Westerlies, 80	Badura et al., 2013
		Danube area (Czech, Austria, Slovakia, Hungary, Croatia , Serbia, Romania, Bulgaria)	Alps (4810) & Carpathian Mountains (1602)	Danube, ~600; and its tributaries	Alluvial plains	Westerlies, 200	Smalley and Leach, 1978; Wright, 2001; Frechen et al., 2003; Smalley et al., 2009; Fitzsimmons et al., 2012; Marković et al., 2016
		Italy	Southern Alps piedmont (4810)	Po, ~150	Alluvial plains; Dried-out shelves;	South-southwesterly winds, 50	Coudé-Gaussen, 1990; Forno, 1990; Busacca and Cremaschi, 1998; Rousseau et al., 2007
		North Caucasus	Caucasus Mountains (5642)	Kuban, ~200; etc.	Alluvial plains	Westerlies, 50	Jefferson et al., 2003a
	Asia	Siberia (Russia)	Altai & Sayan Mountains (4374); Verkhoyanskiy Khrebet (2389), etc.	Tobol; Ishim; Irtysh; Ob, ~600; Yenisei, ~400; Angara, ~150; Lena, ~900; Aldan, ~600; and Kolyma, ~300	River valley; Alluvial plains; Outwash	Westerlies, 100–300	Péwé and Journaux, 1983; Jefferson et al., 2003a; Chlachula, 2003; Smalley et al., 2009; Murton et al., 2015
		Eastern China	Da Hinggan & Yanshan mountains (2029); Mountains in the middle Yellow River (e.g. the Lvliang & Qinling mountains)	Songhua, ~400; West Liaohe, ~400; and Yellow, ~500; etc.	Alluvial plains; Sandy Land; Dried-out shelves; Floodplains	west-southwest winds (Northeast China), 300; North wind (lower Yellow River), 80	Liu et al., 2000; Peng et al., 2007; Prins et al., 2009; Yin and Qin, 2010; Kang et al., 2011; Stevens et al., 2013; Wang et al., 2014; Nie et al., 2015; Zheng, 2018

(*continued on next page*)

Table 1 (*continued*)

Loess genesis mode	Continent	Region	Source area (Highest elevation, m)	River & maximum transportation distance (km)	Main deflation area	Wind & maximum transportation distance (km)	References
		South Asia	Himalayas (~8000)	Indus, 200; Jhelum, 50; Gangetic, 200; and their tributaries	Alluvial fans; Alluvial plains	Northeast or southwest monsoon, 300	Dodonov and Baiguzina, 1995; Pant, 1993; Ahmad and Chandra, 2013; Liu et al., 2017
	Oceania	New Zealand	Tararua & Rimutaka mountains (2797); Southern Alps (3764)	Clutha, Mataura, and Rakaia etc. 50–100	Alluvial plains	Westerlies, 80	Smalley, 1995; Eden and Hammond, 2003; Hesse and Mctainsh, 2003; Smalley et al., 2009; Muhs et al., 2014
MRD Mode	South America	Southern Pampas (Pampa Interserrana) & Pampa Deprimida of Argentina	Andes (34–38° S, 6800); Tandilia and Ventania ranges; Southern Volcanic Zone in Andes	Desaguadero-Salado, ~500; Colorado, ~400; and Negro, ~400	Alluvial plains; Alluvial fans; Steppe	Westerly and southwesterly winds, 700	Sayago et al., 2001; Zárate, 2003; Zárate, 2007; Muhs et al., 2014
	Asia	Central Asia	Tianshan Mountains (7495); Hindu Kush Mountains (7485); Pamirs	Amu Darya, ~500; and Syr Darya, ~500	Sandy Deserts; Alluvial fans; Alluvial plains	Westerly or northerly winds, 600	Dodonov and Baiguzina, 1995; Derbyshire, 2001; Jefferson et al., 2003a; Smalley et al., 2006; Machalett et al., 2006; Dodonov, 2007; Smalley et al., 2009; Machalett et al., 2013; Fitzsimmons et al., 2016
		Loess Plateau of China	Qilian Mountains (5547); Gobi-Altay and Hangayn Mountains (3905)	Heihe, ~300; Shiyang, ~150; Yellow, ~1000; and flash floods of Gobi-Altay Mountains, ~80	Gobi; Badain Jaran Desert, Tengger Desert, Ulan Buh Desert, Hobq Desert and Mu Us Desert; Alluvial fans; Alluvial plains	Northwest monsoon, 800	Liu et al., 1985; Liu et al., 1985; Wang, 1990; Derbyshire, 2001; Sun, 2002a; Gu et al., 2011; Muhs, 2013b; Stevens et al., 2013; Smalley et al., 2014
		Northwestern China	Tianshan (7443), Altai, Kunlun (8611) and Altun (6295) mountains	Tarim and its tributaries, 100–200; Ili, ~400; and other ephemeral streams	Deserts in Junggar Basin, Tarim Basin, Qaidam Basin and Kazakhstan	Northwesterly (Junggar), Northwesterly (Qaidam), Northeasterly (Tarim), and Northwesterly (Ili basin), ~500	Liu et al., 1985; Sun, 2002a, 2002b; Machalett et al., 2006; Porter, 2007; Gu et al., 2011
	Africa & Arabian Peninsula	North of the Sahara (Tunisia, Libyan)	Ahaggar Massif (2918); Tunisian Upland; Atlas Mountains (4165)	Ephemeral streams	Grand Erg Oriental; Alluvial fans; Chotts	Southwesterly winds, 300	Wright, 2001; Crouvi et al., 2010; Muhs, 2013a
		South of the Sahara (Nigeria)	Tibesti (3415), Ennedi, Air, Ahaggar (2918) Massifs; Uplands in south of Sahara	Chari-Logone; and other ephemeral streams	Lake Chad Basin; Bodele Depression; Grand Erg de Bilma	Northeasterly winds, 700	Wright, 2001; Crouvi et al., 2010
		Namibia	Great Escarpment; other uplands (inferred)	Ephemeral streams	Kalahari Sands; Playa	Easterly wind, 350	Eitel et al., 2001; Crouvi et al., 2010
		Israel	Ethiopian highland (4620) & north-eastern African craton; Mountains in southern Sinai Peninsula	Nile, ~1000; Arish, ~200	Northern Sinai - western Negev desert; Dried-out shelf; Wadis	West-southwest winds (Israel), 100	Muhs, 2013a; Crouvi et al., 2008; Crouvi et al., 2010; Ben-Israel et al., 2015
	Oceania	Australia	Flinders Range (1166), Great Dividing Range (2228)	Murray-Darling, ~600; and other ephemeral streams	Sand dunes & playas in Murray-Darling Basin & Lake Eyre Basin	Westerly winds, 700	Dare-Edwards, 1984; Hesse and Mctainsh, 2003; Haberlah, 2007; Smalley, 2008; Greene et al., 2009; Muhs, 2013a; Muhs et al., 2014; Williams, 2015

Notes: The highest elevations of mountains and uplands are taken from Zhou (2011). The maximum distances of major river and wind transportation are estimated using Google Earth satellite map according to the locations indicated by relevant references.

Table 2
Summary of global loess distribution.

Continent	Region	Deposit environment	Thickness (m) General	Thickness (m) Local	Continuity	References
North America	Mid-continent of US	River terraces; Mountain slopes; Plains	< 20	60	Continuous in most areas; discontinuous in some marginal areas	NRCCED, 1952; Grimley, 2000; Bettis et al., 2003; Busacca et al., 2003; Roberts and Muhs, 2007
	Colorado Plateau of US	River terraces; Mountain slopes	< 2	–	Relatively continuous	Bettis et al., 2003
	Palouse region of US	River terraces; Mountain slopes; Basin	< 75	75	Continuous in most areas; discontinuous in some marginal areas	NRCCED, 1952; Bettis et al., 2003
	Snake River Plain of US	River terraces; Mountain slopes	< 2	12		
	Alaska of US	River terraces; Mountain slopes	< 10	~ 100	Continuous in most areas	Busacca et al., 2003; Muhs et al., 2003; Roberts and Muhs, 2007; Muhs, 2013b; Murton et al., 2015; Muhs et al., 2018
South America	Gran Chaco	River terraces; Plains	< 18	–	Relatively continuous	Zárate, 2003; Zárate, 2007
	Tucuman region	Mountains slopes	< 50	~50	Continuous	Zárate, 2007; Muhs et al., 2014
	Uruguay	River terraces; Plains	1–2	–	Unknown	Zárate, 2003
	Northern Pampas	Plains	< 40	~50	Continuous	Zárate, 2007; Muhs et al., 2014
	Southern Pampas	Plains; Mountain slopes;	< 10	–	Continuous	Zárate, 2003
Europe	Western & central Europe	River terraces; Plains; Mountain slopes	< 20	~ 100	Continuous in most areas; discontinuous in some marginal areas	Jefferson et al., 2003b; Editorial board of Dictionary of Earth Sciences, 2006; Haase et al., 2007; Marković et al., 2009; Muhs et al., 2014; Marković et al., 2015; Marković et al., 2016
	Eastern Europe	Plains; Hills; River terraces; Piedmonts	< 20	50	Continuous in most areas; discontinuous between Don River and Volga River	Haase et al., 2007
Asia	Loess Plateau of China	Mountain slopes; River terraces; Basins	< 300	505	Continuous	Wang and Zhang, 1980; Li and Sun, 2005; Lei, 2014
	Northwestern China	Mountain slopes	< 50	~120	Continuous	Wang and Zhang, 1980; Sun, 2002b; Li and Sun, 2005
	Northeastern China	River terraces; Plains; Mountain slopes	< 40	~ 100	Continuous	Wang and Zhang, 1980; Li and Sun, 2005
	Central Asia	Mountain slopes; River terraces	< 70	~ 200	Continuous	Smalley et al., 2006; Dodonov, 2007; Muhs et al., 2014
	South Asia	Mountain slopes; River terraces	< 30	–	Relatively continuous	Dodonov, 2007
	Siberia of Russia	River terraces; Mountain slopes	< 150	–	Continuous in most areas; Unknown in north parts	Chlachula, 2003; Jefferson et al., 2003a,b; Péwé and Journaux, 1983; Murton et al., 2015
Africa & Arabian Peninsula	Tunisia	Mountain area	< 10	20	Relatively continuous	Coudé-Gaussen, 1987; Wright, 2001; Crouvi et al., 2010
	Nigeria	Mountain area	< 2	–	Discontinuous	Coudé-Gaussen, 1987; Wright, 2001; Smith et al., 2002
	Namibia	River terraces; Mountain slopes	< 10	15	Relatively continuous	Eitel et al., 2001, Brunotte et al., 2009
	Israel	Mountain area	< 12	–	Relatively continuous	Ben-Israel et al., 2015
	Yemen	Mountain area	~ < 1	–	Unknown	Nettleton and Chadwick, 1996
Oceania	Australia	Plain	1–3	–	Relatively continuous in western part ; discontinuous in eastern part	Hesse and Mctainsh, 2003; Muhs et al., 2014
	New Zealand	Plains; Downlands; Coasts	0.5–6	~ 20	Continuous in most areas; discontinuous in some marginal areas	Xia et al., 1993; Eden and Hammond, 2003; Muhs et al., 2014

Notes: Thickness are summarized based on main references and maps used for Figure 6.

Smalley and Derbyshire (1990) mentioned that loess is a geographically confined material, thus necessitating a systematic analysis of geographical distribution, specific features within each distinct region, and the origin and transport of loess materials. Wright (2001) proposed moving away from classifying loess deposits according to the source region or type and towards considering the significance of environmental, tectonic, and geomorphological factors at all stages of loess formation.

In this review, we comprehensively summarized the major provenances, river and wind transport paths of major loess areas (Table 1) throughout the world. The spatial distribution characteristics as well as deposition environments of these major loess areas are summarized in Table 2. On large scales of at least hundreds of kilometers, the parameters of preceding processes including source area environments, river transport paths, and the existence of desert transition zones, all exhibit noticeable or remarkable differences, except for the terminal aeolian transport stages, which do not show significant differences. By considering differences in source areas and transportation pathways and the possible existence of desert transition zones, as well as the current and Quaternary environments, the following three modes of loess genesis in the global loess inventory were identified.

(1) Continental glacier provenance-river transport mode (CR mode): The source materials are mainly produced in continental glacier regions with average elevations of only a few hundred metres and then transported by rivers to the middle and lower reaches of the rivers for deflation. No big transition zone exists between the river and the loess deposition area.
(2) Mountain provenance-river transport mode (MR mode): The source materials are mainly produced in relatively high-altitude areas and then transported by rivers to the middle and lower reaches of the rivers for deflation. No big desert transition zone exists between the river and loess deposition area.
(3) Mountain provenance-river transport-desert transition mode (MRD mode): The source materials are mainly produced in high altitude areas and then transported by rivers to their middle and lower reaches or desert basins, where they are deflated. A large sandy desert or land transition zone exists in the long-distance wind transport path from the river to the loess deposit area.

According to the spatial distribution characteristics (Table 1) and the three modes of loess genesis, the global map of loess genesis is compiled as shown in Fig. 1, which shows the source areas and transport paths of major loess accumulation, main mountains, rivers, deserts, Quaternary ice-sheets, and modern 1500 m altitude wind circulation patterns.

2.1. Continental glacier provenance-river transport (CR) mode

The northern parts of North America and Europe both had vast continental ice sheets with thicknesses reaching approximately 3000 m during the Quaternary glacial periods (Dyke et al., 2002; Svendsen et al., 2004). The loess in the Central United States and eastern Europe to the east of the Carpathian Mountains (spanning Ukraine, Belarus, Moldova, and southwest of Russia) (Fig. 1) mainly originated from the marginal zones of these continental ice sheets (Muhs, 2007; Smalley et al., 2009).

The loess area in Central United States was formed primarily with materials from the margins of south lobes of Quaternary Laurentide Ice Sheet (LIS) to the north (Fig. 1). These source materials were mainly delivered by the tributaries of Mississippi River, such as Wabash, Illinois, and Ohio rivers to the south (Grimley, 2000; Bettis et al., 2003; Muhs and Bettis, 2003; Muhs, 2007; Smalley et al., 2009). Secondary source materials came from the Rocky Mountains, and were transported by Platte, Arkansas and Red rivers to the east (Grimley, 2000; Bettis et al., 2003; Roberts and Muhs, 2007; Smalley et al., 2009). The wind direction for the loesses in this region was westerly or northwesterly (Muhs and Bettis, 2000; Roberts and Muhs, 2007; Muhs, 2013a; Schaetzl et al., 2018a).

The primary source area for the eastern Europe loesses was the continental glacier region covered by the southeastern part of the Quaternary Fennoscandian ice sheet in northern Europe (Fig. 1). The source material was transported south to the vast plains and hilly areas by the Dnieper, Don, and Volga Rivers, which drained melting water from the glacier (Jefferson et al., 2003a; Muhs, 2007; Smalley et al., 2009). In addition, some of the upland areas in the middle reaches of these rivers served as secondary sources of material. Wind transport was mainly provided by the prevailing westerlies (trade winds) from the northern Atlantic (Jefferson et al., 2003a). Both the eastern European and the Central United States loess regions had continental glaciers to the north and rivers for southward transportation and loess coverage was extensive and continuous.

2.2. Mountain provenance-river transport (MR) mode

The main source areas of loess deposits formed in this mode were mountains with high altitudes, such as the Alps, Altai Mountains, Alaska Range, Andes, and Southern Alps (Fig. 1). Large active rivers connect the mountainous source areas in the upper reaches to the loess deposits near the middle and lower reaches of rivers. These rivers, including the Rhine, Po, Danube, Dnieper, and Volga Rivers in Europe, Ob and Yenisei Rivers in Siberia, Snake and Yukon Rivers in North America, and Parana River in South America, formed from mountain glacier meltwater and surface runoff. Most loess deposits are located within 200 km (a few as close as 50 km and as far as 300 km) of one or both sides of the middle and lower reaches of these rivers and are either continuously or intermittently distributed between terraces near rivers and even in distant mountain slopes or semi-arid plains.

In terms of global distribution, MR mode-derived loesses are widespread and well-dispersed (Fig. 1). The following section summarizes the characteristics of the main areas of this loess type in Western United States, Alaska, northern Argentina and adjacent regions, Central and Western Europe, Siberia, eastern China, South Asia, and New Zealand.

2.2.1. North America

Located in the Columbia Plateau, the Palouse loess mainly consists of silt from slack water sediments transported by the southwest winds. These sediments were ascribed to the outburst floods of the proglacial Lake Missoula in the Quaternary, which is located in what is now the Columbia River system. The surrounding mountain glaciers contributed to the main original source areas (Bettis et al., 2003; Busacca et al., 2003). Meanwhile, the loess materials in the Snake River plain were transported by the Snake River from the surrounding mountains to the alluvial plain and then were transported by west-northwest winds (Busacca et al., 2003; Roberts and Muhs, 2007). Transport by the San Juan River was responsible for the thin loess deposits in the Colorado Plateau (Bettis et al., 2003). The source areas of these three loess regions were all in the Rocky Mountains. In Alaska, the maximum loess thickness, which is usually found near rivers, indicates that the materials were derived from glaciers in Alaska and Brooks mountain ranges and carried by rivers, such as the Tanana, Yukon, and Colville. The loess silts were wind-blown from the floodplains of braided glacial rivers during the glacial periods or modern outwash plains. The loesses in Central Alaska act as important records of the regional northeast winds during the glacial periods (Péwé, 1975; Busacca et al., 2003; Roberts and Muhs, 2007; Muhs et al., 2018).

2.2.2. South America

Gran Chaco loess (located in northern Argentina, Bolivia, and Uruguay between latitudes 15° to 27° S) was mainly sourced from the upper reaches of the Parapetí, Pilcomayo, and Bermejo Rivers in the Andes Mountains between northwestern Argentina and south of Bolivia

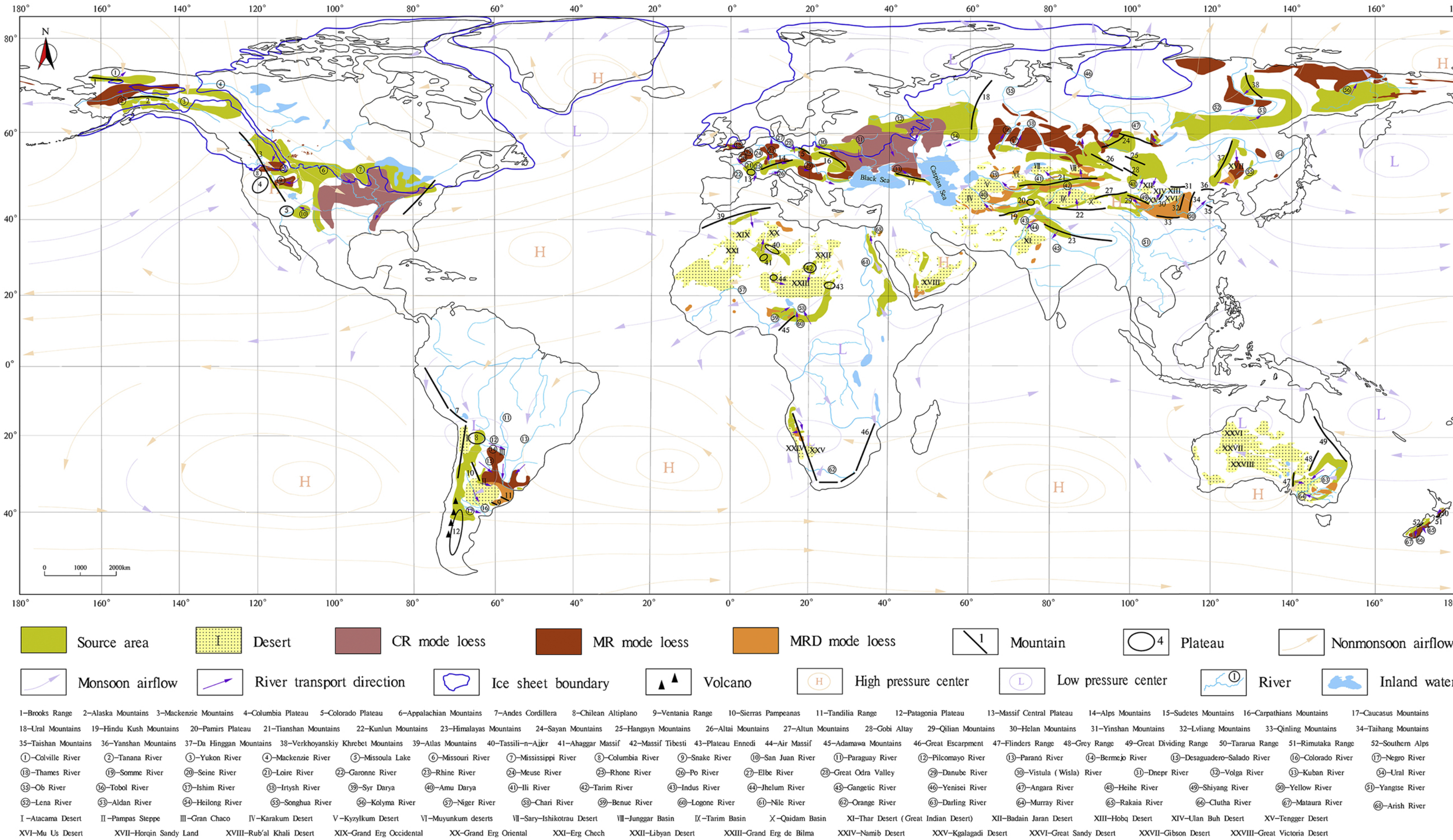

Fig. 1. Global map of loess genesis.

Notes: Universal transverse Mercator (UTM) projection is used. The latitude–longitude grids and global land borders modified from Liu (1965) by including inland waters, rivers, mountains and deserts according to the map in https://maps-for-free.com/. The maximum extents of the Quaternary ice sheets redrawn from Dyke et al. (2002) and Svendsen et al. (2004). Modern wind circulation patterns (streamlines) in boreal winter at 850 hPa (about 1500 m altitude) redrawn and modified from An et al. (2015).

Locations of loess source areas were inferred from the descriptions in these references: *for North America* - Péwé (1975), Grimley (2000), Bettis et al. (2003), Busacca et al. (2003), Muhs and Bettis (2003), Roberts and Muhs (2007), Muhs (2007) and Smalley et al. (2009); *for South America* - Smalley (1995), Iriondo (1997), Sayago et al. (2001), Zárate (2003), Zárate (2007) and Muhs et al. (2014); *for Europe* - Smalley and Leach (1978), Coudé-Gaussen (1990), Forno (1990), Lebret and Lautridou (1991), Busacca and Cremaschi (1998), Wright (2001), Frechen et al. (2003), Jefferson et al. (2003a,b), Hill (2005), Muhs (2007), Rousseau et al. (2007), Antoine et al. (2009), Smalley et al. (2009), Fitzsimmons et al. (2012), Badura et al. (2013), Lehmkuhl et al. (2016) and Marković et al. (2016); *for Asia* - Péwé and Journaux (1983), Liu et al. (1985), Wang (1990), Pant (1993), Dodonov and Baiguzina (1995), Liu et al. (2000), Derbyshire (2001), Sun (2002a), Sun (2002b), Jefferson et al. (2003a), Chlachula (2003), Smalley et al. (2006), Machalett et al. (2006), Peng et al. (2007), Porter (2007), Dodonov (2007), Crouvi et al. (2008), Smalley et al. (2009), Yin and Qin (2010), Crouvi et al. (2010), Gu et al. (2011), Kang et al. (2011), Machalett et al. (2013), Ahmad and Chandra (2013), Muhs (2013a, 2013b), Wang et al. (2014), Smalley et al. (2014), Murton et al. (2015), Ben-Israel et al. (2015), Fitzsimmons et al. (2016) and Liu et al. (2017); *for Africa* - Eitel et al. (2001), Wright (2001), Crouvi et al. (2010) and Muhs (2013a); *for Oceania* - Dare-Edwards (1984), Smalley (1995), Eden and Hammond (2003), Hesse and Mctainsh (2003), Haberlah (2007), Smalley (2008), Smalley et al. (2009), Greene et al. (2009), Muhs (2013a), Muhs et al. (2014) and Williams (2015).

and transported by the north wind from the alluvial plains of these rivers (Iriondo, 1997; Zárate, 2003, 2007). By contrast, the mountain valley loess of Tucuman in Argentina is thought to have been sourced from the Chilean Altiplano of the Andes (Zárate, 2003).

In the Pampa Ondulada of northern Pampas, loess materials mainly came from the Paraná River and its tributaries from the Andes in the west. Secondary sources providing particles include the Sierras Pampeanas (a chain of mountains to the east of and parallel to the Andes Mountains) and metamorphic outcrops located on the Uruguayan margin of the Rio de la Plata (Zárate, 2003, 2007). The prevailing westerly and southwesterly winds account for the loess deposits in the Pampas (Sayago et al., 2001; Zárate, 2007; Schaetzl et al., 2018b).

Most loesses in South America have direct input from volcanic particles from the Andean volcanic eruptions. The volcanoes in the Puna plateau, which are part of the Central Volcanic Zone, are believed to be the main source of the loesses in the Chaco region and some in the northern Pampas tephra (Zárate, 2007; Muhs et al., 2014).

2.2.3. Europe

The topographic elevation differences and directions of large rivers indicate that the Alps, together with the Carpathian Mountains and certain uplands in Central Europe, are the main sources of loess materials for Central and Western Europe, with the continental glacier area to the north being only a secondary source (Hill, 2005; Smalley et al., 2009). During the major glacial periods in the Quaternary, large-scale glaciers were present in the Alps. Mountain glacial sources and transportation by glacier melt rivers are therefore major characteristics of the loesses in these regions (Svendsen et al., 2004; Smalley et al., 2009; Marković et al., 2016).

The braided river valleys and a broad belt of land, now submerged in the English Channel and North Sea, are believed to be the main wind deflation areas from which some of the loesses in northwestern France, Belgium, southeastern England, and northern Germany were blown (Koster, 1988; Lebret and Lautridou, 1991; Jefferson et al., 2003b; Hill, 2005; Haase et al., 2007; Antoine et al., 2009; Badura et al., 2013; Lehmkuhl et al., 2016). Loess materials were carried to these deflation sites by rivers, such as the Somme and Seine of France, Meuse River of Belgium, Thames of England, proto-Rhine that once turned westward into the English Channel, Elbe River, and Great Odra Valley that once turned westward into the North Sea due to blockage by ice sheets. The riverbeds and alluvial plains of some inland rivers also served as local deflation areas for many loess deposits near these rivers. These rivers, in addition to those mentioned above, include the Loire, Garonne, and Rhone Rivers of France (Coudé-Gaussen, 1990; Lebret and Lautridou, 1991; Rousseau et al., 2007; Smalley et al., 2009; Muhs et al., 2014), Vistula (Wisla) River of Poland that flows from the Carpathian Mountains (Badura et al., 2013), and Po River of Italy (Coudé-Gaussen, 1990; Forno, 1990; Busacca and Cremaschi, 1998).

The upper reaches of the Danube River received Alpine materials, while the middle reaches received materials from the Carpathian Mountains and other uplands. The Danube River also carried some Fennoscandia glacier materials through the Moravian Depression. The river bed and alluvial plains served as wind deflation areas for many loesses near the Danube River (Smalley and Leach, 1978; Wright, 2001; Frechen et al., 2003; Smalley et al., 2009; Fitzsimmons et al., 2012; Marković et al., 2016). The source materials of the loesses north of the Caucasus Mountains in southeastern Europe were transported by rivers from these mountains (Jefferson et al., 2003a).

North of the Alps was mainly influenced by the north Atlantic air mass during the Quaternary glacial periods, bringing the prevailing westerlies along the latitude 50° N corridor with increased continentally towards the east (Rousseau et al., 2007; An et al., 2015; Marković et al., 2016). Apart from the westerlies, northwestern Europe also experienced various local winds, such as the strong northwest winds in France, Germany, and Poland, because of cyclones that made important contributions to the deposition of northwestern European loess (Lebret and Lautridou, 1991; Renssen et al., 2007; Antoine et al., 2009; Badura et al., 2013). South of the Alps was appreciably conditioned by the Mediterranean climate (Marković et al., 2016), where the south-southwest winds brought in the aeolian loess in Italy (Forno, 1990). The loess in the middle and lower Danubian basins in Central Europe was mainly transported by the westerlies (Marković et al., 2016).

2.2.4. Asia

The source materials of the loesses in southwestern Siberia originated from the southern mountains and were delivered by several river systems to the northern plains and then transported by wind to the zones between the mountains and plains slightly south. These river systems from west to east include the Tobor River, Ishim River from the southern uplands, Irtysh River from the Altai Mountains, Ob River, Yenisei River from the Altai and Sayan Mountains, and the Angara River, which is the only outlet of the Baikal that delivers materials from the mountains on its both sides, such as the Baikal Range (Jefferson et al., 2003a; Chlachula, 2003; Smalley et al., 2009). The provenance function of the upper reaches of the Ob River was also improved by meltwater erosion during the glacial periods by periodic cataclysmic outbursts from large ice marginal lakes in the north, which lead to flooding of the southern portion of West Siberia, and from ice-dammed lakes in the adjacent Altai Mountains (Chlachula, 2003).

In northeastern Siberia, the Central Yakutian Lowland is surrounded by the Verkhoyansk Khrebet Mountains to the north and several mountain ranges to the east and south, all of which contained glaciers during the glacial periods, and to the west by the Quaternary continental glacier region. The source materials from these surrounding areas were carried by the Lena River and its tributaries (e.g., the Aldan River), which were fed by glacial meltwater and then transported by wind from the outwash and alluvial plains of these rivers (Péwé and Journaux, 1983). By contrast, the hypothesized sources of loess in the Kolyma lowland are sediments from the eastern and southern uplands that were delivered by the palaeo-Kolyma River and its glacially sourced tributaries to the Khallerchin tundra to the north and exposed shelf of the East Siberian Sea for deflation (Murton et al., 2015). The westerlies traveling between the southwest and northwest directions were prevalent in Siberia for most of the Pleistocene as they are currently. These winds played an important role in loess distribution across this region (Derbyshire, 2001; Chlachula, 2003; An et al., 2015).

Loesses in Northeast China came from different sources. The northern regions were sourced from the local Da Hinggan Mountains and other mountains, where the materials were carried by the Songhua River and other rivers and wind-blown in the spring by west and southwest winds (Kang et al., 2011). Loesses in the southern parts originated from the southern foot of Da Hinggan Mountains and northern foot of the Yanshan Mountains, which are both adjacent to Horqin Sandy Land. The materials delivered by the West Liaohe River to the Horqin Sandy Land were then blown eastward to the loess accumulation area (Yin and Qin, 2010; Kang et al., 2011). For the loess in the Central Shandong Province, the primary dust sources were transported by the north wind from the proximal alluvial plains of the lower Yellow River and the once-exposed shelf of the Bohai (sea) Gulf (Liu et al., 2000; Peng et al., 2007; Wang et al., 2014; Zheng, 2018). The materials on the alluvial plains and the shelf of the Bohai Gulf were supplied by the Yellow River carrying materials from Lvliang and Qinling Mountains (Ren, 2006; Stevens et al., 2013; Nie et al., 2015).The long-range transported dust that blew from the northwest deserts of China via the westerly winds was a secondary source (Liu et al., 2000; Peng et al., 2007; Wang et al., 2014). Some loess was deposited in the Mangshan Plateau to the southeast of the Loess Plateau, on the south bank of the Yellow River, and about 100 km downstream of Sanmen Gorge, where the dust source was the proximal Yellow River floodplains (Prins et al., 2009; Stevens et al., 2013).

Meanwhile, the loess in the uplands north of the Indo-Gangetic Plain in South Asia mainly originated from the Himalayas. The particulate materials were carried by the tributaries of the Indus and Ganges Rivers to the deflation area in the upstream region of these rivers. The Thar Desert to the west served as a secondary dust source (Pant, 1993; Dodonov and Baiguzina, 1995; Liu et al., 2017). The main source area of the loess in Kashmir to the north was the local mountains, where the materials where carried by local rivers, such as the Jhelum River, and then redeposited by wind (Pant, 1993; Dodonov and Baiguzina, 1995). In addition, Ahmad and Chandra (2013) noted the secondary contribution of dust transported over a long range by the westerlies. Pant (1993) believed much of the loess in South Asia was delivered by the northeast winter monsoon during the glacial periods. However, Liu et al. (2017) believed that, unlike loesses in the majority of other areas of the world that were formed through the influence of winter winds, the source materials of loesses southwest of New Delhi were delivered by the southwest summer monsoons.

2.2.5. Oceania

The loess deposits adjacent to the Rangitikei, Manawatu, and Wanganui Rivers in the North Island of New Zealand came from non-glacial mountain areas (e.g., Tararua and Rimutaka Mountains) in the central part of the region. Materials for these deposits were carried by the aforementioned rivers to the floodplains downstream and shelves that were previously exposed during the Quaternary and then transported by the westerly winds. Meanwhile, the sources of loesses found near volcanoes on the central North Island originated from wind-blown volcanic sediments (Eden and Hammond, 2003; Muhs et al., 2014).

In the South Island, the Southern Alps were typical glacial source areas during the Quaternary glacial periods. These source materials were mainly transported by the Mataura, Clutha, and Rakaia Rivers southeast to the alluvial plains and the once-exposed shelves and then wind-blown to the adjacent plains and downlands (Smalley, 1995; Eden and Hammond, 2003; Smalley et al., 2009; Muhs et al., 2014). Some loesses in the northern and eastern parts of the island were blown from local fans and eroding faces of mountainous areas (Eden and Hammond, 2003).

2.3. Mountain provenance-river transport-desert transition (MRD) mode

Loess deposits created via this mode tend to be distributed at low latitudes or in inland regions, where are more arid than MR mode loesses (Fig. 1). The main source areas can be mountains that still have glaciers at high altitudes, such as the Qilian and Tianshan mountains in China, as well as dry and rocky mountains or uplands with medium altitudes, such as the Gobi Altai Mountains north of China and several plateaus in the Sahara of Africa. Large areas of sandy deserts or sandy lands are observed along the transport pathways. Adjacent mountains or uplands generally supply a large amount of the source materials over a long period of time via surface runoff to these semi-enclosed desert basins. Rivers can be formed by glacial meltwater from the high-altitude mountains or floods due to short-term precipitation in arid mountains. As a result of the arid environment, some regions are unable to form large rivers; thus some fluvial transport is by ephemeral rivers with lower discharge than those involved in the MR mode of genesis.

Deflation areas include vast deserts, floodplains, piedmonts, and even mountainous source areas exposed to prevailing near-ground winds. The average aeolian transport distances from the river banks or desert centres to the centres of the loess areas can be 700 km or greater. The desert region acts as a transition zone or transfer station. The formation of a desert transition zone is mainly the result of particles being sorted by size during long-period and long-distance large-scale wind transport in the arid regions (Wright, 2001; Sun, 2002a; Muhs, 2013b). The loess deposits formed via this mode are relatively continuous and thick in China, Central Asia, and South America, but dispersed and thin in Africa, the Arabian Peninsula, and Australia. The regional descriptions of these loess areas are as follows.

2.3.1. South America

The loesses in the Pampa Interserrana subregion (southern Pampas) and Pampa Deprimida subregion (eastern part of the northern Pampas) primarily originated from the 34°-38° S section of the Andes (Sayago et al., 2001; Zárate, 2003, 2007; Muhs et al., 2014), with the Southern Volcanic Zone of the mountain range serving as the main tephra source (Zárate, 2007; Muhs et al., 2014). There were also minor and localized contributions from the Tandilia and Ventania Ranges located southeast of the Pampas (Zárate, 2003). The source materials from the Andes were transported to the floodplains downstream by the Negros and Colorado Rivers and Desaguadero-Salado fluvial system (a tributary of the Colorado) (Fig. 1) and then transported by west-southwest winds. A vast sand transitional area formed southwest of the Pampas. Although weak vegetation exists in this sand area at present, it was an arid desert in Quaternary (Zárate, 2007).

2.3.2. Asia

In Central Asia, the loess source materials were generated from the Tianshan Mountains and western edge of the Tibetan Plateau (Pamirs). These materials were delivered by the Syr Darya and Amu Darya Rivers to the deflation sites, which consist of proluvial fans, floodplains, and the Karakum and Kyzylkum deserts from east to west, with the distribution direction being essentially parallel to the general river direction (Jefferson et al., 2003a; Dodonov, 2007; Smalley et al., 2009). These deserts served as transfer stations for the source materials (Smalley et al., 2006). Aeolian transport of silt dust for final deposition onto the east piedmonts mainly occurred via the west and northwest winds due to a combination of the weakening of the westerly from the North Atlantic and Mediterranean and strengthening of the Siberian-Mongolian anticyclone and Asiatic polar front from the north in the glacial periods (Dodonov and Baiguzina, 1995; Derbyshire, 2001; Machalett et al., 2013; Fitzsimmons et al., 2016).

In China, the primary source areas of the Loess Plateau include the Qilian Mountains on the northeast edge of the Tibetan Plateau (Wang, 1990; Derbyshire, 2001; Sun, 2002a; Gu et al., 2011) and the Gobi-Altai and Hangayn Mountains in southern Mongolia (Sun, 2002a). The loess materials from the Qilian Mountain were carried to the edge of the Badain Jaran, Tengger and Mu Us deserts by the Heihe, Shiyang and Yellow rivers and surface runoff of many other proluvial fans that were mainly fed by glacial meltwater (Wang, 1990; Gu et al., 2011; Stevens et al., 2013). Materials from the Gobi Altai and Hangayn Mountain were carried by precipitation-induced short-term floods to the fans and Gobi (stony and gravel deserts) north of the Badain Jaran Desert (Sun, 2002a). Under the influence of the Mongolian-Siberian high-pressure system during the winter and spring, the strong northwest near-surface wind (Asian monsoon) generated by Mongolian cyclones was the primary influencer of loess formation in the Loess Plateau (Liu et al., 1985; Derbyshire, 2001; Sun, 2002a; Muhs, 2013b). The northwest to southeast zonation with a decreasing mean particle size from the Gobi to the sandy desert to the loess is due to sorting of particle materials by the long-distance wind (Liu et al., 1985; Sun, 2002a). The sand dusts blown from the Badain Jaran Desert bypassed the Helan Mountain barrier and went further to the Ulan Buh Desert to the north and Tengger Desert to the south. Silt particles of suitable size were blown to the Mu Us Desert and then to the Loess Plateau across the Yellow River (Liu et al., 1985; Stevens et al., 2013). These vast deserts along the material transport pathway acted as transition zones or transfer stations, as well as secondary provenances (Sun, 2002a; Gu et al., 2011; Smalley et al., 2014).

The loess at the boundaries of the three inland basins (Junggar, Tarim, and Qaidam Basins) in northwestern China originated from the surrounding high mountains, including the Altai, Tianshan, Kunlun, and Altun Mountains. The mountainous source materials were transported by glacial meltwater to the fans and then wind-blown to the Gobi in front of the mountains and deserts in the center of each basin (Sun, 2002a,b; Porter, 2007). The directions of the prevailing near-surface winds in the Junggar, Tarim, and Qaidam Basins were northwest, northeast, and northwest, respectively (Liu et al., 1985; Sun, 2002a,b; Gu et al., 2011). The loess around the Ili Basin was sourced from the Tianshan Mountains. The materials were transported west through the Ili River and then transported from the Sary-Ishikotrau Desert in Kazakhstan by the northwest winds (Sun, 2002b; Machalett et al., 2006).

2.3.3. Africa and Arabian Peninsula

The loesses in Tunisia and Libya north of the Sahara Desert and the discontinuous loess zone in the Sahel region south of the Sahara Desert are derived from dusts from the Sahara Desert (Crouvi et al., 2010). However, these materials originally came from uplands inside deserts, including the Ahaggar, Tibesti, Ennedi, and Air Massifs, and mountains along the margins. These materials were transported by ephemeral streams from the dry uplands inside the deserts and by rivers from the outer mountains to sabkhas, alluvial fans, wadis, chotts, and vast deserts for later deflation (Wright, 2001; Muhs, 2013a; Williams, 2015). The Lake Chad Basin and Bodele Depressions east of Nigeria were typical places of accumulation of materials transported by rivers. Particle comminution during fluvial transport and salt weathering in these accumulation sites further contributed to silt generation (Wright, 2001). Aeolian dust transport proceeded southwestwards in Tunisia, southwards in Libya, and northeastwards in the Sahel region. The northeasterly Harmattan winds through Sahel, which still prevail today in this region in winter and are major dust winds internationally, also cause surface soil erosion into the Atlantic Ocean (Crouvi et al., 2010; Muhs, 2013a).

For the loess in northwest Namibia between the Great Escarpment to the coast, westward seasonal rivers brought some materials from the Great Escarpment (mountains). Dusts were carried by easterly winds partly from these river valleys, as well as from the western Kalahari Desert east of the Great Escarpment (Eitel et al., 2001; Crouvi et al., 2010). The particle sources of the Kalahari Desert may be the low mountains around the desert basin.

Compared to other loess areas with large desert transition zones (e.g., Chinese loess), the sub-Saharan loess in Africa is scarce. The reasons for this may include the following: (1) a lack of the massive amount of materials required from glacial or montane sources (Pye, 1995); (2) the presence of zones with thick vegetation, which are conducive to the retention of dust close to the source, were rare (Pye, 1995); (3) a lack of mountain barriers between the desert and sea that would prevent dust from flowing to the sea; (4) an unstable Quaternary climate in this region that did not allow dust supply and wind transport routes for loess formation to last long enough (Pye, 1995); (5) the transformation during the late Quaternary of the climate of the area south of the Sahara region to hot and humid, which caused some loess to become weathered or modified (Pye, 1995); and (6) the remobilization of a significant amount of freshly deposited dust (over 40%) by strong wind or water during the same season that the dust was deposited (Pye, 1995; Wright, 2001; Smith et al., 2002).

For Israel loesses located in northern and central Negev, the main dust sources were the Sinai-Negev deserts in the northern Sinai Peninsula and western Negev and dried-out Mediterranean shelf during low sea-level periods and were transported by west-southwest winds (Muhs, 2013a; Crouvi et al., 2010; Ben-Israel et al., 2015). The distant Sahara and Arabia deserts could be minor dust sources for the fine silts of the Negev loesses (Ben-Israel et al., 2015). The Sinai-Negev sands mainly came from the Nile delta, as well as the wadis of the seasonal Arish River which flowed to northern Sinai (Crouvi et al., 2008; Ben-Israel et al., 2015). The original particle sources have not been fully studied. Perhaps the Ethiopian highland and north-eastern African craton were washed by the Nile River (Ben-Israel et al., 2015) and mountains in the southern Sinai Peninsula were washed by the Arish River.

2.3.4. Oceania

The loess materials in southeastern Australia were derived from physical weathering of the eastern uplands, such as the Flinders Range (Haberlah, 2007; Greene et al., 2009; Williams, 2015). These materials were then transported by rivers to the relict lakes, playas, and salinas in the inland drainage depocentres, such as the Lake Eyre and Western Murray-Darling River Basins, as well as to seasonal inland river floodplains. Subsequently, many large area of transition sands have been formed on the wind transport pathways in the arid Quaternary (Dare-Edwards, 1984; Hesse and Mctainsh, 2003; Haberlah, 2007; Greene et al., 2009; Muhs, 2013a). The Great Dividing Range, the source of the Murray-Darling Rivers, was also a potential source (Smalley, 2008). Aeolian transport was by the westerlies through southern Australia, which also blew some dust into the Tasman Sea and even New Zealand (Eden and Hammond, 2003; Hesse and Mctainsh, 2003; Greene et al., 2009; Muhs et al., 2014).

3. Loess distribution

Aeolian transportation is followed by the deposition of silt-size grains and accumulation of loess in semi-arid regions with favorable geomorphologic conditions (Table 2) and climate (Pye, 1995; Muhs, 2013a). Reduction of and separation by grain size are ongoing processes. Coarse sand grains (200–600 μm in diameter) are moved by saltation and deposited close to the source, loess (silt-size) grains (20–60 μm) travel medium-distances near the surface in short-term suspensions and are deposited in sheltered areas, and long-range transport dust (typically < 10–20 μm) is easily carried in long-term suspensions at high elevations and therefore does not easily accumulate in certain areas (Smalley, 1966; Pye, 1995; Mason et al., 1999; Muhs and Bettis, 2003; Smalley et al., 2009; Muhs, 2013a; Vandenberghe, 2013; Luehmann et al., 2013). This is why the silt and clay fractions become finer in loesses as the distances to the deflation source areas increase (Ulrich, 1950; Liu et al., 1985; Muhs and Bettis, 2003). Pye (1995) emphasised that the accumulation of extensive thick loesses requires (1) a large and sustained supply of suitably sized particles and (2) a suitable downwind trap (often a well-vegetated surface sheltered by a topographic barrier). Such areas of loess accumulation may include (1) a well-vegetated surface adjacent to a dust source, (2) a vegetated semi-arid margin of desert a certain distance from sandy zone where proximal to sediment source, (3) an area joined to proximal (relative to sediment source) sand dunes and sheets by a transitional sandy loess zone (Pye, 1995), and (4) an area beyond or against topographic barriers, such as mountain ranges with varying heights (Schaetzl and Loope, 2008; Lehmkuhl et al., 2016). Deposited aeolian sediments can be stabilized by reducing wind and water erosion through vegetative cover and moderate moisture (Pye, 1995; Smalley et al., 2011). In some areas, primary loesses become reworked and redeposited by slope processes or running water, thereby becoming secondary loesses, i.e., loess-like deposits or loess derivatives (Liu et al., 1985; Pye, 1995; Dodonov, 2007).

This section discusses the spatial (geographic) occurrence, thickness, continuity, and areal extent of loess deposits in different continents/regions, generally moving from the western to eastern hemisphere and then from north to south within each hemisphere. As will be noted, Asia, particularly China, is afforded a more lengthy discussion due to the availability of plentiful references. As Muhs (2013b) pointed out, no continent has received more attention in terms of loess research than Asia.

3.1. Spatial distribution

Loesses are scattered across arid and semi-arid regions in the middle latitudes of the northern and southern hemispheres. Previous descriptions and maps of the major loess regions around the world mostly have incomplete coverages at small scales. These include, but are not limited to, NRCCED's (1952) 1:2,500,000-scale aelian deposit map of North America, Zárate's (2007) descriptive summary of South American loesses, Haase et al.'s (2007) 1:2,500,000-scale loess map of Europe, Liu's (1965) 1:4,000,000-scale loess map of China, Dodonov's (2007), and Muhs et al.'s (2014) sketch maps of Central Asian loesses, Crouvi et al.'s (2010) sketch map of loesses across African and the Arabian Peninsula, Eden and Hammond's (2003) sketch map of New Zealand loesses, and Muhs' (2013b) and Muhs et al.'s (2014) sketch maps of loesses in South Asia, Siberia, and Australia.

These selected sources provide relatively comprehensive and detailed information on the distribution of loesses on continental and regional scales, but differ significantly in terms of their compilation dates and degrees of detail. In this study, relatively new literature has been compiled and sorted to confirm and improve the distributions and descriptions for some localities around the world. For example, NRCCED's (1952) highly detailed map on the loess distribution in the United States lacks proper descriptions, as well as loess occurrences in Alaska; therefore, Bettis et al.'s (2003) detailed descriptions of the continental USA and Murton et al. (2015)'s work on Alaska were consulted. Haase et al. (2007) compiled several sources with different standards, which resulted in some problems, including omission of local loess-covered areas (Lehmkuhl et al., 2016). These problems were addressed by incorporating Jefferson et al.'s (2003b) study on loess distributions in England and Lehmkuhl et al.'s (2016) and Solarska et al.'s (2013) studies in Germany and Poland. The relatively brief information on the loess distribution in Siberia reported in the schematic maps by Muhs (2013b) and Muhs et al. (2014) was expanded based on the works of Chlachula (2003) and Jefferson et al. (2003a) on Central Siberia and Péwé and Journaux (1983) and Murton et al. (2015) on Northeast Siberia. Although Liu's (1965) map was based on extensive field investigations, Liu et al. (1985) proposed updating it as new data were gathered, which has not yet been attempted. In particular, the distributions of loesses in the lower reaches of the Yangtze River and western Sichuan were incorporated from works by Yang et al. (1988) and Liu (2009). A schematic map of Derbyshire (2001) was used to supplement the map of the loess distribution in South Asia by Muhs et al. (2014).

Differences between the various sources for maps of loess distributions in South America are obvious. For example, the sketch map by Smalley et al. (2009) considered most of the Pampas as covered with loess, while Muhs et al. (2014) and Zárate (2007) considered the northeast of the Pampas to be covered by loess and the southwest to be a transitional sandy land. Zárate's (2007) map, which integrates different subregional maps with better detail and accuracy, was used as a reference in this study. The scale of Crouvi et al.'s (2010) map of the loess in Africa and the Arabian Peninsula is relatively small with no precise boundaries of some small loess areas. Eitel et al.'s (2001) map was used in this study to verify the distribution of loesses in Namibia. The loess map of Africa and the Middle East by Muhs (2013b) was also used to verify the loess distribution. The schematic map of Australian loesses by Muhs et al. (2014) was compiled from Hesse and Mctainsh (2003) and contains some conjectural elements. Smalley (2008) mentioned that the loess distribution in Australia still needs to be mapped in moderate detail.

Based on the above references, this study presents an updated global loess distribution map (Fig. 2) that uses the Polyconic Projection with the meridional interval on the same parallel decreasing away from the central meridian by equal difference. It also contains rivers, waters, national boundaries and loess continuity, and improves the precision of global loess maps, such as the maps by Pye (1987) and Li and Sun (2005).

As shown in Fig. 2, most loesses are found in the mid-latitude arid to semi-arid regions of both the northern and southern hemispheres. Extensive loesses are found in North and South America, Europe, and Central and northern Asia, while smaller deposits can be found in Africa, the Arabian Peninsula, Australia, and New Zealand. The distributions of loesses in different regions are discussed in more detail below. The accompanying descriptions of the regional loess distributions emphasize provenances and transport pathways and utilize large mountains and rivers as the main geographical references.

3.1.1. North America

Most of the loesses in North America are located south of the margins of the Laurentide and Cordilleran ice sheets, which existed during the last glacial period, extending further south to the lower Mississippi River Basin. Loesses are also present in the Colorado and Columbia Plateaus in the northwestern contiguous United States and Alaska (Bettis et al., 2003; Muhs et al., 2014).

The most extensive loess deposit is in the midcontinent region; specifically, it is in the Great Plains and Central Lowland along the Missouri-Mississippi River Basin and east of the Mississippi Plain (NRCCED, 1952; Roberts and Muhs, 2007; Muhs et al., 2014). This loess area is approximately 1000 km wide (Grimley, 2000).

In the Colorado Plateau located in southwestern Colorado and southeastern Utah, there is an extensive area of thin loess mapped northeast of the San Juan River. Southwest of the river, there are large deposits of aeolian sand and silt (NRCCED, 1952; Bettis et al., 2003). In the Columbia Plateau, there is around 50,000 km^2 of loess distributed in the Palouse region with large tracts also found along both sides of the river in the Snake River Plain (NRCCED, 1952; Bettis et al., 2003).

The loesses in central Alaska are widely distributed along mountain slopes, terraces, and lowlands near major rivers, such as the Yukon and Tanana. Much of the loess on the north- and northeast-facing slopes has remained frozen following deposition during the Pleistocene. In northern Alaska, a special type of loess, called yedoma or “ice complex” that is similar to that found in Siberia, is distributed north of the Brooks Range roughly parallel to the Colville River. Yedoma refers to ice- and carbon-rich silts and silty sand deposits penetrated by large ice wedges formed from sedimentation and syngenetic freezing during the late Pleistocene (Muhs et al., 2003; Schirrmeister et al., 2013; Murton et al., 2015; Muhs, 2013b; Muhs et al., 2018). East of Alaska, ice-rich loesses similar to Siberian yedomas are found in many valleys southwest of the Yukon region in Canada. Many places near rivers originating from mountain glaciers continue receiving loess materials and forming Holocene loess (Murton et al., 2015).

3.1.2. South America

The loesses in South America are mainly found in the Pampas of Central Argentina and Gran Chaco region of northern Argentina, Bolivia, and Paraguay. The eastern part of the Pampas contains the continent's most extensive and continuous loess belt, which runs about 900 km from north to south. In the Gran Chaco region, the distribution is also wide, but dispersed mainly in the plains of the Parana River Basin and eastern piedmonts and intermountain basins of the Sierras Pampeanas (Zárate, 2003, 2007; Muhs et al., 2014).

Some smaller distributions are present in neighboring areas, particularly in southwestern Bolivia, western Paraguay, southern Brazil, and western Uruguay (Zárate, 2007; Muhs et al., 2014). Additionally, loesses have been reported, but have not yet been mapped, in Tierra del Fuego, some eastern piedmonts of the Andes, and the edge of the Atacama Desert in Peru (Muhs et al., 2014).

3.1.3. Europe

Most of the loesses in Europe are found near the foothills and lower mountain belt north of the Alps and the Carpathian Mountains, as well as in the Danube Basins and vast plains of eastern Europe (Haase et al., 2007; Muhs et al., 2014). In Western and Central Europe, the loess belt is located at about 50° N latitude between the margins of the Fennoscandian ice sheet to the north and glaciers on the Alps to the south and mainly traverses France, Belgium, Germany, and Poland. Here, the loess zones, which range between 10 and 200 km wide, are scattered across plains (Northwest France), piedmonts, river terraces, and basins. In the

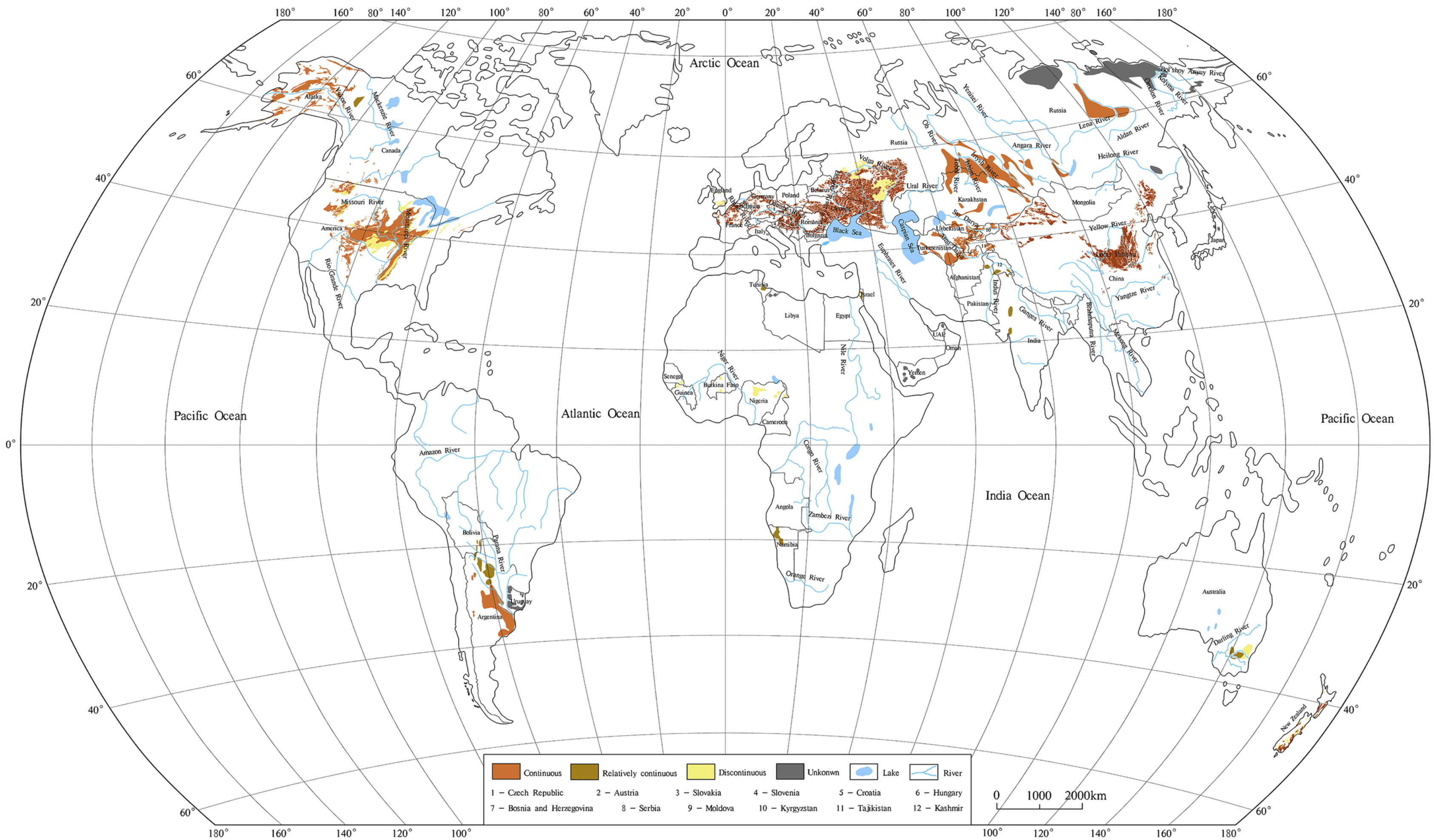

Fig. 2. Global loess distribution and continuity.

Notes: Main references for this map include: *for North America -* NRCCED (1952), Bettis et al. (2003) and Murton et al. (2015); *for South America -* Zárate (2007); *for Europe -* Haase et al. (2007), Jefferson et al. (2003b), Solarska et al. (2013) and Lehmkuhl et al. (2016); *for Siberia-* Péwé and Journaux (1983), Chlachula (2003), Jefferson et al. (2003a), Muhs (2013b), Muhs et al. (2014) and Murton et al. (2015); *for China -* Liu (1965); *for Central Asia -* Dodonov (2007) and Muhs et al. (2014); *for South Asia -* Muhs et al. (2014) and Derbyshire (2001); *for Africa and Arabian Peninsula –* Crouvi et al. (2010) and Muhs (2013b); *for Australia -* Muhs et al. (2014); *for New Zealand -* Eden and Hammond (2003) and Muhs (2013b).

Danube Basins, a large loess area is located in the Middle Danubian Plain south of the Carpathian Mountain arch that mainly covers parts of Austria, the Czech Republic, Slovakia, Hungary, Croatia, and Serbia (Marković et al., 2009, 2015, 2016). This intermittently distributed loess zone is approximately 300–400 km wide from north to south. Loess is also found in the Lower Danube Basin between the Carpathian and Balkan Mountains in southern Romania and northern Bulgaria.

Meanwhile, the largest loess area in eastern Europe is bounded to the west by the Carpathian Mountains, to the east by the Ural Mountains, to the south by the Black Sea and Caucasus Mountains, and to the north by the southern margin of the Quaternary Fennoscandian ice sheet (now the Smolensk-Moscow Upland). This loess is distributed across Ukraine, Belarus, Moldova, and Southwest Russia (Jefferson et al., 2003a) in the plains and a few hilly areas along the Dnieper, Don, and Volga Rivers. The north-to-south width of the loess belt ranges from 400 to 1200 km.

Outside of these major areas, loess zones are also found scattered in southern England (Jefferson et al., 2003b), near the Rhone and Garonne River Valleys in France, and in the Italian Po River Valley. There is also minimal loess found in Spain, southern Italy, and the southern Balkans that has not yet been mapped (Haase et al., 2007).

3.1.4. Asia

3.1.4.1. Siberia. Large deposits of loess are found in southwestern Siberia, where they are generally located in the basins and tributaries of the Ob and Yenisei Rivers. These basins are located north of the Altai and Sayan Mountains, east of the Ural Mountains, and west of the Angara River. The loess zone measures approximately 1500 km from north to south (Chlachula, 2003; Jefferson et al., 2003a). In the northeast, loesses are present in the Central Yakutian Lowland in the Lena River Basin and the Kolyma Lowland in the Kolyma River Basin (Péwé and Journaux, 1983; Murton et al., 2015).

The Ob (Priobie) Plateau west of the Ob River and Kuznetsk Depression east of the Ob River have the thickest loess deposits in Siberia. Loesses are also present in the basins of the Ishim, Tobol, and Irtysh Rivers. All of these rivers flow into the Ob River. The loess in the upper reaches of the Yenisei Valley is found in the Northern Minusinsk Depression. Along the artificial Krasnoyarsk Lake (reservoir), the loess profile is approximately 400 km long. Upstream of the Angara River, loess deposits are located along the river valley near Irkutsk (Chlachula, 2003; Jefferson et al., 2003a).

In northeastern Siberia, there are yedoma silt deposits. In the Central Yakutian Lowland west of the Okhotsk Sea, loesses are present in the upland terraces and low plateaus in Central and Southern Yakutia along the Lena River and its tributary, the Aldan River, above the permafrost (Péwé and Journaux, 1983; Murton et al., 2015). Loesses are widely spread along the Kolyma Lowland south of the East Siberian Sea and west of the Kolyma River with its southern boundary stretching onto the alluvial plains to reach the frontier of the adjacent uplands. Some loesses also appear in low mountainous areas in the southern and western regions of the Kolyma Lowland.

3.1.4.2. Central and South Asia. The loesses in Central Asia are mainly concentrated on the windward slopes of the Central Asian Orogenic Belt, which includes the Tianshan, Kunlun, Hindu Kush, and Pamir Mountains (Dodonov, 2007; Muhs et al., 2014). Most deposits are found in the area bounded to the west by the Pamirs and Tianshan Mountains and to the east, by the Karakum, Kyzylkum, and Muyunkum deserts. Covering the piedmonts and foothills along the Amu Darya and Syr Darya, these deposits traverse the countries of Uzbekistan, Kyrgyzstan, southern Kazakhstan, Tajikistan, and Turkmenistan, as well as parts of northern Afghanistan (Dodonov, 2007; Muhs et al., 2014).

In South Asia, specifically India and Pakistan, loess zones are mainly scattered in the uplands to the south of the Hindu Kush Mountains and Himalayas, as well as along some mountain valleys in Kashmir and Siwalik foothills (Dodonov, 2007). Some sporadic distributions are also observed in the upper reaches (northern part) of the Indo-Gangetic Plain (Liu et al., 2017).

3.1.4.3. China. The loesses in China are mainly between the Altai-Yinshan-Da Hinggan mountain chain to the north and Kunlun-Qinling mountain chain to the south and effectively form an intermittent loess belt from west to east with the Chinese Loess Plateau in the middle of the belt (Fig. 2). The eastern end divides into two branches: the northern branch, which turns to the Songliao Plain in northeastern China, and the southern branch, which turns to the Shandong Peninsula and the middle and lower reaches of the Yangtze River, e.g., Nanjing (Liu, 1965; Yang et al., 1988). Outside of this loess belt, scattered distributions are found in the western Sichuan Plateau and Chengdu in southwestern China (Yang et al., 1988; Liu, 2009).

In northwestern China, loesses are mostly found on the margins of the Tarim and Junggar Basins and cover the north and south piedmonts of the Tianshan Mountains, western edge of Junggar Basin, and north piedmont of the Kunlun Mountains. Some loess deposits also developed on the southeast edge of Qaidam Basin and Hexi Corridor north of the Qilian Mountains (Liu, 1965).

The loess region in the middle reaches of the Yellow River in Central China is bounded by the Wushao Mountain in Gansu Province to the west, Taihang Mountains to the east, Qinling Mountains to the south, and Great Wall to the north. The width from north to south is approximately 700 km and west to east is approximately 1200 km. This region contains the thickest loess and most complete loess strata in China (Fig. 3) (Liu, 1965; Wang and Zhang, 1980; Liu et al., 1985). Specifically, the thick loess between the Liupan and Lvliang Mountains, as well as even the Taihang Mountains, almost completely covers the tertiary and other old rock strata, leaving only several bedrock mountain tops exposed to form distinctive loess landforms, and hence the name "Loess Plateau" (Liu et al., 1985). Typical loess landforms include loess platforms (yuan, in Chinese), ridges (liang), hillocks (mao), columns (zhu), bridges (qiao), and walls (qiang). The first three are grouped as first-order loess landforms (Fig. 4) (Zhang, 2000; Zhu et al., 2009), while the last three (Fig. 5), developing within first-order landforms, are grouped as secondary loess landforms (Fuller, 1922;

Fig. 3. Typical loess strata in China: (a) a 40 m high loess-paleosol profile (taken in Yuci, Shanxi in 2018); and (b) a road cut slope exposing 80 m high loess-paleosol accumulation (taken in Jixian, Shanxi in 2017).

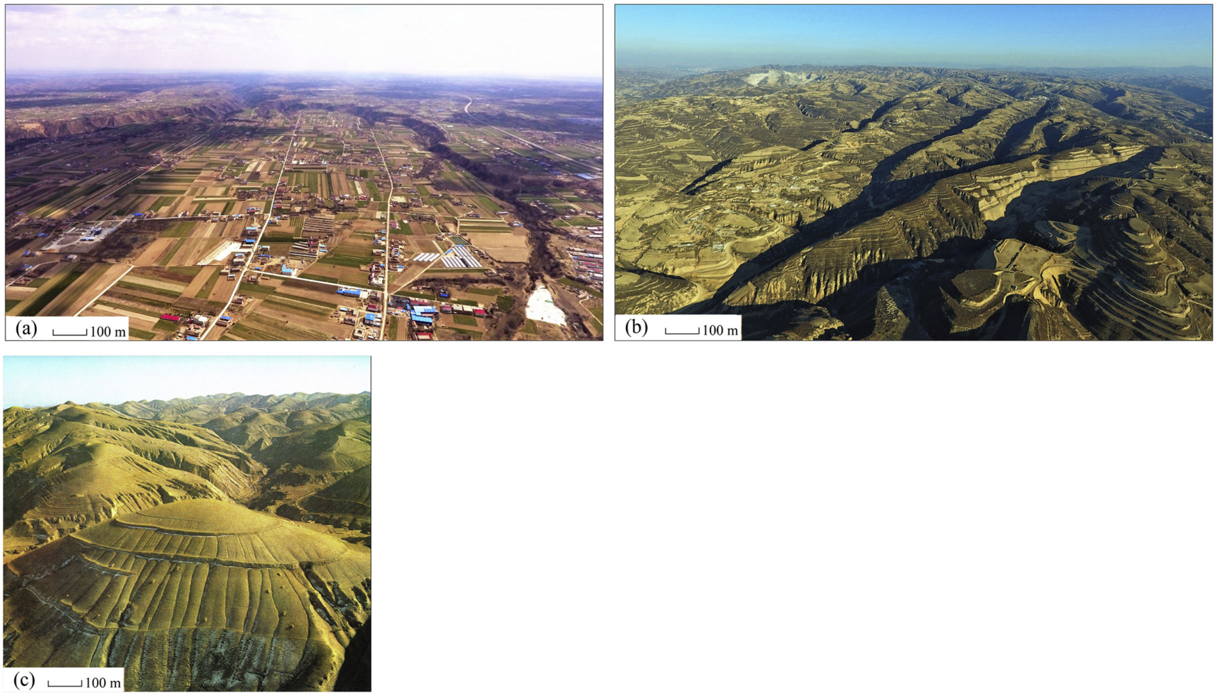

Fig. 4. Typical first-order loess landforms in China: (a) loess platform (taken in Xifeng, Gansu in 2017); (b) loess ridge (Liulin, Shanxi in 2016); and (c) loess hillock (Baiyushan, Shaanxi, Wang and Zhang, 1980).

Zhang, 1983; Sun, 2005).

The loesses in eastern China are mostly found in the foothills and plains. In northeastern China, the loesses are widely distributed along the Songliao Plain of the Songhua and Liaohe river basins, as well as in the adjacent eastern mountainous areas. Around the North China Plain, the loesses are mostly distributed in the piedmonts and river terraces south of the Yanshan Mountain, east of the Taihang Mountains, and east of the Qinling Mountains. There are large areas of secondary loess deposited alternately with other alluviums in the North China Plain, but these have not been considered or mapped as loess regions. The loesses in the Shandong Province are found in the Taishan and Lushan piedmonts and the piedmonts and intermontane basins of the northern Shandong Peninsula. Some loesses are also distributed along the northern part of the Haihe River Plain and some parts of the Yellow River Plains (Liu, 1965; Wang and Zhang, 1980; Li and Sun, 2005).

3.1.5. Africa and the Arabian Peninsula

Loesses in Africa and the Arabian Peninsula do not have as widespread a distribution as in other continents. The African loesses are mainly scattered in the northern part and south of the Sahara Desert, as well as in Namibia. In the Arabian Peninsula, loesses are mainly found in Israel and Yemen (Crouvi et al., 2010; Muhs et al., 2014).

In northern Sahara, loesses are found in the Matmata Plateau in South-Central Tunisia and to the north of the Tripolitanian Plateau in Northwest Libya. These two loess regions are approximately 250 km apart (Wright, 2001; Crouvi et al., 2010). Small loess regions have also been reported, but have not been mapped, in Morocco, Algeria, and the Canary Islands (Muhs, 2013b). South of the Sahara in the Sahel region, the most well-known loess deposit is the Zaria loess in the Kano Plains in Central-Northern Nigeria (Crouvi et al., 2010; Muhs et al., 2014). These deposits were for a long time called “drift soils” (Coudé-Gaussen, 1987). Scattered reports from other Sahelian countries also indicate the presence of a discontinuous loess belt distributed from west to east in the Cape Verde Islands, southern Senegal, Guinea, Mali, Burkina Faso, Niger, and northern Cameroon that has not yet been mapped (Crouvi et al., 2010; Muhs, 2013b). Further to the south in northwestern Namibia, loess deposits are found between the edge of the Great Escarpment highland and northern Namib Desert, where they fill basins or are along seasonal river terraces (Eitel et al., 2001; Crouvi et al., 2010).

In the Arabian Peninsula, the most prominent loess lies in the arid Negev region of southern Israel, where it meets the western desert, covers the bedrock in the north, and fills in the depressions and valleys

Fig. 5. Typical secondary loess landforms in China: (a) loess column (taken in Yuci, Shanxi in 2016); (b) loess bridge (Ruicheng, Shanxi, Wang and Zhang, 1980); and (c) loess wall (Luochuan, Shaanxi in 2017).

in the central uplands of the region (Eitel et al., 2001; Crouvi et al., 2010). In Yemen, loesses are found in the western Sanaa-Dhamare-Taizz plateaus and arid valleys of the Sadah region in the northwestern part of the country. A small number of loesses that has yet to be mapped is also found in front of the Oman Mountains in the northeastern United Arab Emirates (Crouvi et al., 2010), as well as in Syria and Iraq (Yang and Liu, 2008).

3.1.6. Oceania

The loess distribution in Australia was once widely thought to be limited. Butler (1956) first used the term "parna" to refer to a type of aeolian clay in Southeastern Australia and differentiate it from loess. Today, many scholars consider it a special clay-rich loess (Dare-Edwards, 1984; Hesse and Mctainsh, 2003; Greene et al., 2009). Parna is found along the southern and eastern margins of the Riverine Plain in the Murray-Darling River Basins, about 300 km from the sand dunes on its western side (Hesse and Mctainsh, 2003; Muhs et al., 2014). The relative rarity of loess accumulation in Australia may be due to strong wind erosion of pre-existing soil surfaces (Dare-Edwards, 1984; Hesse and Mctainsh, 2003) and the lack of barriers keeping dust from being blown to the sea, similar to what occurs in the Sahara of Africa.

In New Zealand, the loesses are widely distributed in certain river terraces, coastal platforms, downlands, and hills of both the North and South Island, particularly downwind of the floodplains (Eden and Hammond, 2003; Muhs et al., 2014). The loesses on the North Island are located in the Manawatu region in the southwest part of the island and inland basins near Hawke's Bay to the east. Meanwhile, the loesses in the South Island are located in Canterbury Plain and surrounding areas in the east part of the island, the Banks Peninsula, and the Otago downlands and Southland Plains in the south part of the island (Muhs et al., 2014).

3.2. Thickness

The current regional maps and literature provide minimal information about the values and variations in thickness across loesses. The major sources of information on loess thickness include (1) a 1:2,500,000-scale map by NRCCED (1952) with a highly accurate depiction of the thickness (up to 10 m) and continuity of loess in the conterminous United States, (2) schematic maps compiled by Bettis et al. (2003) showing variation in thickness for loesses from the last glacial period (Peoria loess) in Central United States, (3) a 1:2,500,000-scale European loess map by Haase et al. (2007) indicating two thickness ranges (2–5 m and > 5 m), (4) a schematic map by Smalley et al. (2006) of parts of Central Asia, (5) a map by Wang and Zhang (1980) of the loess thickness in China, and (6) a map by Eden and Hammond's (2003) of New Zealand showing loess areas with two thickness categories (> or < 1 m). All of these sources of information have been combined into a single global map of loess thickness as shown in Fig. 6.

Note that the reliability of the reference maps of loess deposit thickness is highly variable depending on the availability and quality of the source data. To overcome this problem, a large amount of information scattered across numerous literature sources on loess thickness was collected and sifted through to define typical distribution ranges and maximum thicknesses in each loess region (Table 2) that could then be directly compared with the global loess thickness distribution. The thicknesses of loesses across the world's major loess areas are summarized below.

3.2.1. North America

Most of the loess deposits in the Central United States are no > 20 m thick, with the thickness generally decreasing as the distance from rivers increases (NRCCED, 1952). The thickest deposit reaches 60 m and is found near the Platte River, a tributary of the Missouri River, and Missouri River in the Northwestern Great Plains (NRCCED, 1952; Roberts and Muhs, 2007). Most of the loess deposits in the region are Peoria loess, which makes up > 90% of the total profile thickness in many places (Pye, 1987). Also known as Peoria Silt, Peoria Formation, Peorian loess, and Wisconsin loess (Bettis et al., 2003; Roberts and Muhs, 2007), this loess was deposited during the last glacial period.

The thicknesses of most of the loesses in the Colorado Plateau are no > 1 m, although deposits > 2 m thick are found in some parts (Price et al., 1988; Bettis et al., 2003). In the Columbia Plateau, the loess thicknesses vary from just a few centimeters to tens of meters. The thickest is found in the Palouse region, which is as thick as 75 m (Bettis et al., 2003; Roberts and Muhs, 2007). Some loesses in the Snake River Plain can reach 12 m, but most deposits are no > 2 m thick (Bettis et al., 2003).

Most of the Alaskan loess is < 10 m thick, although deposits as thick as 50–100 m have been observed in some places, including near the Tanana and Yukon Rivers (Busacca et al., 2003; Roberts and Muhs, 2007; Murton et al., 2015). Generally, the thickness of the loess deposit increases as the distance to rivers decreases. The loess deposits in the adjacent Yukon region of Canada are thin and discontinuous (Murton et al., 2015).

3.2.2. South America

The loess in the Gran Chaco plains is not continuous and often interbedded with alluvium. In the northwestern part of the region, the loess deposit is grouped under the 18 m thick Urundel Formation (Zárate, 2003; Zárate, 2007). In Sierras Pampeanas of the Tucumán Province, the mountain loess is 40–50 m thick (Zárate, 2007; Muhs et al., 2014).

In the Pampas, the thickest deposit is about 40–50 m and located in the northern region (Muhs et al., 2014). Along the Chapadmalal sea cliffs, loess sections with heights of 20–30 m are exposed for several kilometers (Zárate, 2007). The loess thickness gradually decreases as it transitions to the southwest sandy land. In the Southern Pampas, deposits are 5–10 m thick in the low mountainous areas and 1.5–2 m in the interfluves (Zárate, 2003).

The loess deposits in Tierra del Fuego and Uruguay are 0.1–1.2 and 1–2 m thick, respectively (Zárate, 2003).

3.2.3. Europe

Most loesses in Europe are < 20 m thick (Editorial board of Dictionary of Earth Sciences, 2006), except for the deposits in the middle and lower reaches of the Danube River (Marković et al., 2015). In Western Europe, the thickest deposits are most likely in Germany in Nussloch (10 km south of Heidelberg) of the Upper Rhine Area (Muhs et al., 2014) and Koblenz of the Middle Rhine Area (Boenigk and Frechen, 2001) with profile thicknesses of 18 and 24 m, respectively.

In Central Europe, the Cerveny Kopec profile of the loess in the Czech Republic in the middle reaches of Danube is 75 m thick, the Krems profile in Austria is 48 m thick (Kukla, 1975; Li and Sun, 2005), the Hungarian loess is 20–29 m thick (EBDES, 2006; Yang and Liu, 2008), and Mošorin section in Serbia is 47.3 m thick (Marković et al., 2015). Romania and Bulgaria in the lower reaches of Danube may have the thickest loesses in all of Europe, with the usual thickness being tens of meters and even exceeding 100 m in northern Bulgaria (Haase et al., 2007).

The thickness of the loesses in the eastern European plains increases from the north edge, where deposits are generally < 2 m thick, to the south, where deposits can be 10–20 m thick, particularly the large loess area at the northern shore of the Black Sea (Haase et al., 2007). This loess area reaches 30–50 m thick in some parts (Dodonov et al., 2000).

Most loesses in south-central England are only 0.3–1 m thick. In Southeast England, some loess deposits > 1 m thick can be found, while South Essex has loess deposits that are 8 m thick (Jefferson et al., 2003b).

3.2.4. Asia

3.2.4.1. Siberia. In Central Siberia, the loess thickness generally

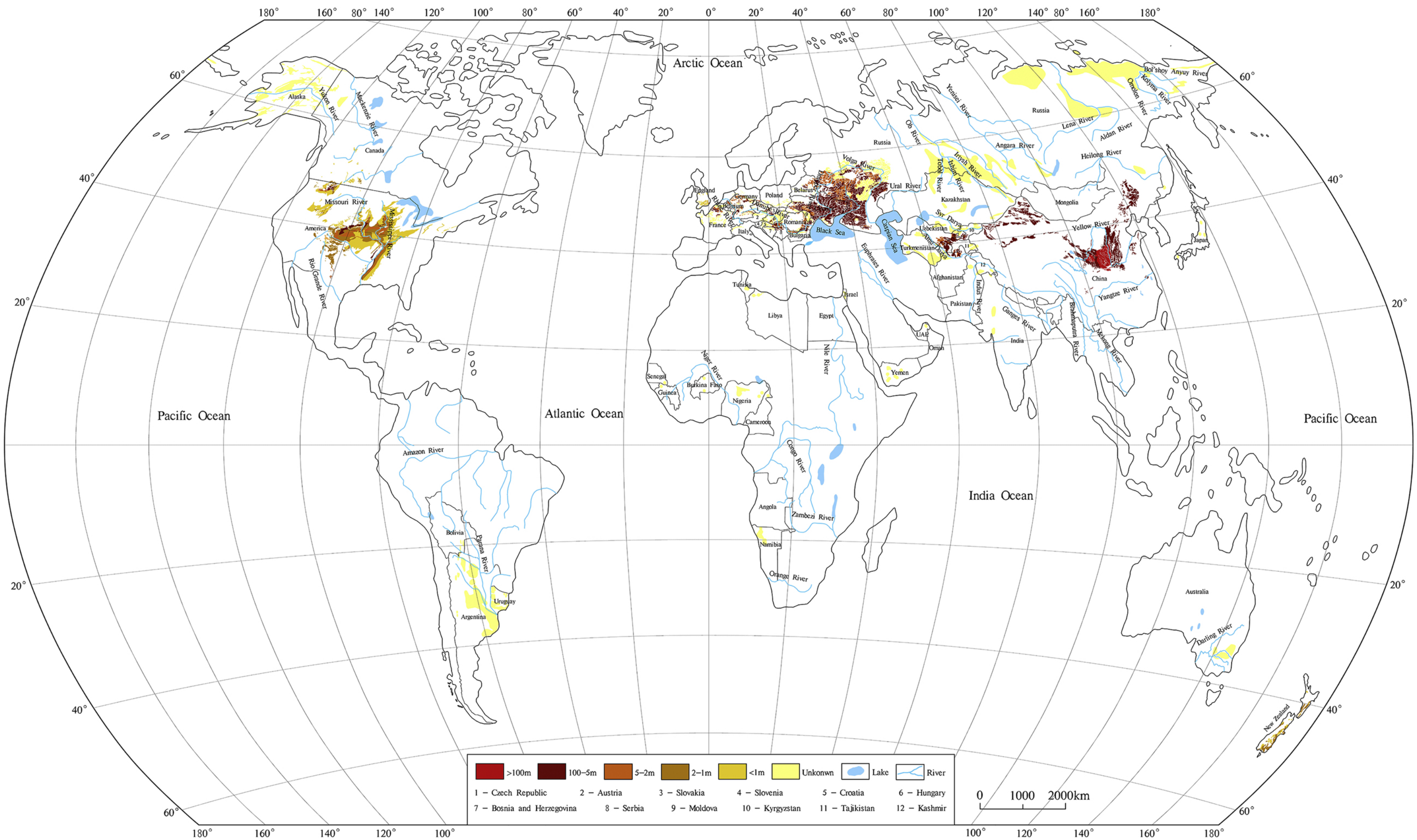

Fig. 6. Global loess thickness distribution. Main references: *for North America* - NRCCED (1952), *for Europe* - Haase et al. (2007), *for China* - Wang and Zhang (1980), *for Central Asia* - Smalley et al. (2006), *for New Zealand* - Eden and Hammond (2003).

decreases from the Ob River Basin moving to the east. In the Ob (Priobie) Loess Plateau and Kuznetsk Depression near the Ob River, the profile can reach 150 m. The maximum thickness of the loess at the west bank of the Yenisei River is 40 m. The loess in the Angara River Basin in the Baikal Lake region is generally 5–20 m thick (Chlachula, 2003).

In Northeast Siberia, the thickest profile, which is near the junction of the Aldan and Lena Rivers in the Central Yakutian Lowland, is as thick as 60 m, whereas the loess deposits in the west side of the Lena Valley are 10–25 m thick (Péwé and Journaux, 1983; Murton et al., 2015). The thickness of the Kolyma Lowland loess varies from a few to tens of meters.

3.2.4.2. Central and South Asia. The thickness of the loess in Central Asia generally increases from several meters at the edge of the western deserts to tens of meters near the eastern mountains west of the Pamirs and western piedmonts of Tianshan. The thick loess deposits are concentrated in Southern Tajikistan, Southern Uzbekistan (Amu Darya drainage basin), and Eastern Uzbekistan (Syr Darya drainage basin), with the thickest deposit reaching 200 m (Smalley et al., 2006; Dodonov, 2007; Muhs et al., 2014). The loess deposits in the Fergana Valley of the Eastern Uzbekistan range in thickness from several to 40 m (Smalley et al., 2006).

In South Asia, the thickness of the loess deposits south of the Hindu Kush Mountains ranges from several to 20–30 m, while those in the loess areas in the Kashmir valley are about 20–30 m (Dodonov, 2007).

3.2.4.3. China. The loess thickness varies widely in different regions of China, with the thickest found in the middle reaches of the Yellow River (Fig. 7). For instance, the loess deposit from the west of the Liupan Mountain to the vicinity of Lanzhou is 200–300 m thick (Wang and Zhang, 1980; Li and Sun, 2005). The thickest loess deposit in China, as well as the world, is located in the Ruoli Township of Jingyuan County, Gansu Province and contains Quaternary loess that is 505 m thick (Lei, 2014). From the Liupan Mountain going east to the Lvliang Mountains, the loess thickness is about 100–200 m (Wang and Zhang, 1980; Li and Sun, 2005).

In the northwest, the deposits in the northern piedmonts of the Qilian and Altun mountains are generally < 50 m thick. In the northern piedmonts of the Kunlun Mountains, the loesses in the foothill terraces are 40–50 m thick, while those covering slopes are generally < 2–3 m thick. The loess deposits in the northern piedmonts of the Tianshan Mountains are generally 10–50 m, while those in the Big Youerdusi Basin in the mountain are 120 m. The loess in the Ili valley is generally 20–60 m thick (Wang and Zhang, 1980; Sun, 2002b; Li and Sun, 2005). In Northeast China, the loess deposits in the southwestern parts and Songliao Plain are about 100 and 40 m, respectively. The loess in the North China Plain, which alternates with other alluviums, is not very thick (Wang and Zhang, 1980; Li and Sun, 2005). In Southwestern China, the loess deposits in the Western Sichuan Plateau are 50–100 m thick (Liu, 2009).

3.2.5. Africa and the Arabian Peninsula

The loesses in Tunisia cover the interfluve area in the Western Matmata Plateau, often filling valleys and small basins > 10 m deep, and has a thickness that sometimes exceeds 20 m (Coudé-Gaussen, 1987; Wright, 2001; Crouvi et al., 2010). Nigeria's Zaria loess is thinner, often only being a few meters thick (Coudé-Gaussen, 1987; Wright, 2001). Smith et al. (2002) also mentioned the existence of “drift deposits” of aeolian origin > 2 m thick in Nigeria. In Namibia, the loesses are generally a few meters thick, with some places having deposits about 15 m thick (Eitel et al., 2001; Brunotte et al., 2009).

The thickness of loesses in the Negev region of Israel ranges from several to about 10 m (Dan, 1990; Crouvi et al., 2008; Ben-Israel et al., 2015). Nettleton and Chadwick (1996) suggested the thickness of the loess deposit near Sanaa of Yemen, which is usually < 1 m, may represent the typical thickness of the local loess.

3.2.6. Oceania

Australian loess deposits are usually 1–3 m thick, although they are occasionally thicker (Hesse and Mctainsh, 2003; Muhs et al., 2014). Meanwhile, the thickness of loess deposits in New Zealand ranges from 0.5–6 m, but 3–4 m is the most common. The maximum known thickness is about 20 m. Loess deposits < 1 m thick are usually adjacent to or at an interphase with > 1 m thick deposits, particularly at the western edges of loess areas in the eastern South Island (Xia et al., 1993; Eden and Hammond, 2003; Muhs et al., 2014).

3.3. Continuity

In the existing literature, there are two types of information on the continuity of loess coverage: (1) maps and quantitative descriptions about continuity (e.g. NRCCED, 1952; Haase et al., 2007; Eden and Hammond, 2003), and (2) qualitative descriptions of the continuity using terms such as “continuous,” “discontinuous,” “sparse,” “fragmentary,” “patchy,” and “sporadic.”

The North America aeolian deposits map by the NRCCED (1952) classified loess coverage according to thicknesses of > 32, 16–32, 8–16, 4–8, < 4, and < 2 ft and continuity as land coverage of > 67, 33–67, and < 33%. Based on this map, continuity is positively correlated with thickness. Most of the sections with loess coverage of < 33% have thicknesses of < 4 ft (about 1.2 m). Sections with > 32 ft (about 9.8 m) thick usually have coverage of > 67%. The map by Eden and Hammond (2003) classified loess cover in New Zealand into “nearly continuous mantle > 1 m” and “mantle < 1 m and/or patches > 1 m.” No further information was provided.

Due to the limited information available, the continuity of loess coverage for the entire world can only be tentatively, rather than accurately classified (Fig. 2; Table 2). Loess deposits in North America (NRCCED, 1952; Bettis et al., 2003; Murton et al., 2015), the Pampas of South America (Zárate, 2007), Europe (Haase et al., 2007; Rousseau et al., 2007), Central and South Siberia of Russia (Péwé and Journaux, 1983; Chlachula, 2003; Jefferson et al., 2003a; Murton et al., 2015), Central Asia (Smalley et al., 2006; Dodonov, 2007; Muhs et al., 2014), China (Wang and Zhang, 1980; Liu et al., 1985; Sun, 2002b; Li and Sun, 2005), and the southern part of the North Island and the eastern and southern parts of the South Island of New Zealand (Eden and Hammond, 2003) are continuous. However, some areas in the margins of these occurrences may be discontinuous.

The loess occurrences in Colorado Plateau of Nouth America (NRCCED, 1952; Bettis et al., 2003), Gran Chaco of South America (Zárate, 2003; Zárate, 2007), South Asia (Dodonov, 2007; Liu et al., 2017), Israel (Crouvi et al., 2008; Ben-Israel et al., 2015), Tunisia (Wright, 2001; Crouvi et al., 2010), Namibia (Eitel et al., 2001, Brunotte et al., 2009), and the western half of the Australian loess area (Muhs et al., 2014) are relatively continuous.

Areas of discontinuous loess exist mainly in (1) the big east and south margins of the Missouri-Mississippi river loess deposits in North America (NRCCED, 1952), (2) South-Central England (Jefferson et al., 2003a, 2003b), (3) the areas between the Don and Volga Rivers of eastern Europe (Haase et al., 2007), (4) the loess belt along the southern region of the Sahara Desert (Crouvi et al., 2010), (5) the eastern half of the Australian loess deposit (Muhs et al., 2014), and (6) the central region of the South Island of New Zealand (Eden and Hammond, 2003).

The continuity of some loess regions is unknown, such as the loess areas in Uruguay, North Siberia of Russia, Libya, and Yemen, as well as many other small sporadic loess areas that have not yet been mapped.

3.4. Areal extent

There have been numerous studies suggesting that primary and secondary loess deposits together cover about 10% of the global land

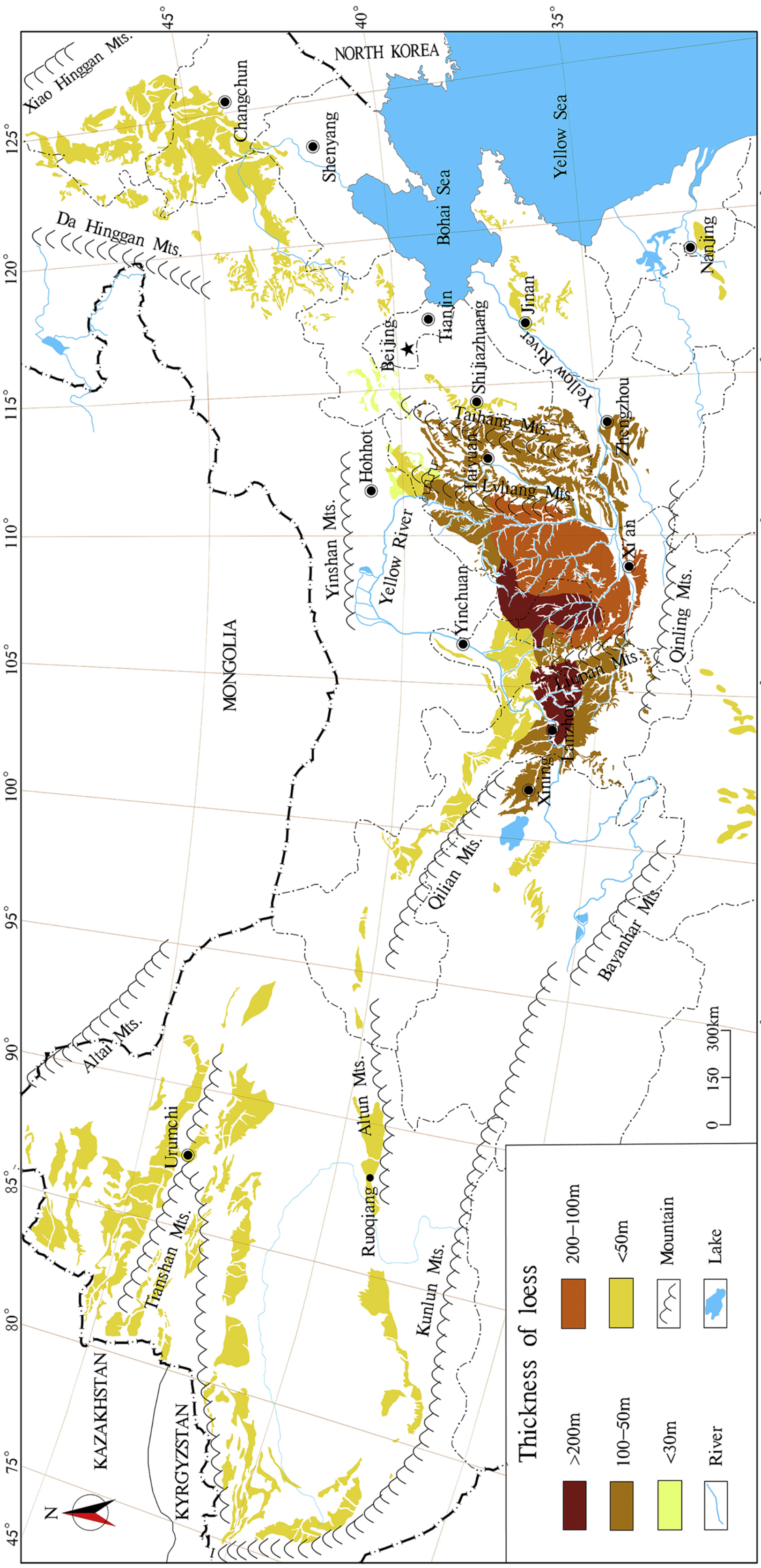

Fig. 7. Chinese loess thickness distribution, modified from Wang and Zhang (1980).

Table 3
Estimated area of main loess regions around the world.

Continent	Country	Area (km^2)	References
North America	Alaska	349,270	Murton et al., 2015
	Canada	46,100	
	USA (Mid-continent)	1,112,610	NRCCED, 1952
	Subtotal	1,507,980	
South America	Argentina	384,420	Zárate, 2007; Muhs et al., 2014
	Bolivia	5350	
	Uruguay	67,280	
	Subtotal	457,050	
Europe	Austria	14,750	Haase et al., 2007
	Belarus	31,420	
	Belgium	9770	
	Bosnia and Herzegovina	7250	
	Bulgaria	21,140	
	Croatia	18,640	
	Czech Republic	12,800	
	France	77,090	
	Germany	63,340	
	Hungary	58,380	
	Italy	5330	
	Moldova	24,420	
	Poland	16,040	
	Romania	40,690	
	Russia (European part)	937,300	
	Serbia	16,650	
	Slovakia	6170	
	Slovenia	1010	
	Ukraine	324,790	
	UK	22,700	Jefferson et al., 2003b
	Subtotal	1,709,680	
Asia	China	635,280	Liu, 1965; Liu et al., 1985
	Russia (Siberia)	3,002,190	Jefferson et al., 2003a; Muhs et al., 2014
	Afghanistan	54,390	Muhs et al., 2014
	India	54,120	
	Kazakhstan	543,200	
	Kyrgyzstan	41,050	
	Pakistan	16,940	
	Tajikistan	71,000	
	Turkmenistan	143,640	
	Uzbekistan	141,650	
	Israel	5500	Crouvi et al., 2010
	Yemen	8160	
	Subtotal	4,717,120	
African	Libya	6800	Crouvi et al., 2010
	Namibia	35,000	
	Nigeria	41,000	
	Tunisia	1300	
	Subtotal	84,100	
Oceania	Australia	76,650	Muhs et al., 2014
	New Zealand	53,070	Eden and Hammond, 2003; Muhs et al., 2014
	Subtotal	129,720	
Global total		8,605,650	

area (e.g., Pécsi, 1968; Pye, 1987; Pécsi, 1990; Wright, 2001; Muhs and Bettis, 2003; Li and Sun, 2005; Muhs, 2007; Solarska et al., 2013; Sprafke and Obreht, 2016). However, these studies all quoted previous estimates using unknown methods.

Based on the newly composed global loess map (Fig. 2), we re-estimated the areal extent of the major loess regions in the world as listed in Table 3. Our estimate of the total area of known loess deposits in the world is about 8,605,650 km^2, which constitutes about 6% of the global land area. Estimates for each distinct loess area (Table 3) were obtained by using MAPGIS program. The small areas with sporadic loess occurrences that have not been incorporated into Fig. 2 could not be included in this estimate. Despite this shortcoming, the total areal extent may have been overestimated due to the small scale and lack of precise information on continuity in most reference maps for composing Fig. 2.

4. Summary and conclusions

This paper presents a systematic and unifying overview of the genesis, distribution, thickness, continuity, and areal extent of all known loess deposits across the globe.

Taking into consideration the provenances and transport pathways of the major loess regions and whether desert transition zones are present, three loess genesis modes, continental glacier provenance-river transport (CR) mode, mountain provenance-river transport (MR) mode, and mountain provenance-river transport-desert transition (MRD) mode, were identified. The updated global loess map presented in this paper treats large mountains and rivers as the main landmarks by which to describe the sources and spatial distributions of loesses (Figs. 1 and 2). The loess thickness (Table 2; Fig. 6) and continuity (Table 2; Fig. 2) are also delineated and the areal extents of loesses (Table 3) in different regions of the world were computed. The following summarizes the scope and conclusions derived from this review:

(1) The source materials for the CR mode of genesis originate from continental glacial regions. Surface erosion caused by the advancement and retreat of ice sheets produces particle materials, which are subsequently transported by rivers to the middle and lower reaches of the rivers for deflation. No big desert transition zone is observed between rivers and areas of deposition. This mode occurred for loesses found in the Central United States and eastern Europe (Fig. 1), where both are characterized with a northern Quaternary continental glacier provenance and large river flowing south, distributing the source materials to vast areas in their middle and lower reaches.
(2) The source materials for the MR mode are generated at high-altitude mountains and are transported to the middle and lower reaches by river for deflation. No big desert transition zone is observed between the river and areas of deposition. Loesses generated via this mode are widely distributed and found mostly in semi-arid areas that are more humid and perhaps colder compared to the areas where MRD mode loesses were generated. These areas include Western United States, Alaska, Northern Argentina and adjacent areas, Central and Western Europe, Siberia, parts of Eastern China, South Asia, and New Zealand. In all these regions, rivers carry particles the entire length of their basins (from the piedmont pluvial fan to the estuary and even to the dried-out shelf during the Quaternary) for deflation. Most river transportation distances range from 200 to 600 km, with a few reaching 1000 km and receiving additional materials in the middle reaches. Loess deposits are found along the rivers, mostly within 200 km (ranging from 50 to 300 km) of the middle and lower reaches of the main rivers. The relatively small distance from the rivers is likely due to the limited wind power or obstruction of terrain barriers.
(3) The source materials for the MRD mode are produced in relatively high-altitude areas and transported by rivers to the middle and lower reaches of the rivers or enter desert basins for deflation. The wind transport pathways from the rivers to the loess deposition areas include large (generally > 200 km) deserts (or sandy land) as transition zones. This loess mode is mainly found in Argentina's Pampas, Central and Western China, Central Asia, Africa, the Arabian Peninsula, and Australia. Compared with the other types, the MRD-mode loess is concentrated in more arid regions in the middle and lower latitudes or inland regions. The large transport distance may be due to stronger winds or absence of terrain barriers. The average aeolian transport distance from a river or a desert centre to the centre of loess deposition areas can reach 700 km or more. The formation of a desert transition zone is the result of particle sorting by long-distance aeolian transport in arid region.
(4) In terms of geographical settings, loesses are intermittently distributed in arid and semi-arid regions in the middle latitudes of the northern and southern hemispheres. Loess deposits can be found at

altitudes ranging from several metres near the coasts (such as in Argentina and New Zealand) to 5300 m north of the Kunlun Mountains of China (Sun, 2002b). Loess is generally found above the groundwater table, except for the frozen water-rich loess in northeastern Siberia and northern Alaska.

(5) The thickest (generally between tens to 300 m thick and reaching a maximum of 505 m) and most continuous loess deposits in the world are located in China (Figs. 6 and 7; Table 2). The thicknesses of the loesses in Siberia and Central Asia are usually tens of metres to < 200 m thick. The thicknesses of the loesses in Europe and North America typically do not exceed 20 m, but reach dozens of metres or close to 100 m in places (e.g., the Lower Danube River, Palouse Region, Nebraska, and Alaska). The loess thicknesses are generally < 50 m in South America, < 20 m in New Zealand, Africa, and the Arabian Peninsula, and < 3 m in Australia.

(6) The largest area covered by loess in the world is located in Asia, with loesses in Europe, North America, and South America following (Table 3). The loess coverage ratios are approximately 16.6% for Europe, 10.6% for Asia, 6% for North America, and 2.6% for South America. Globally, loesses cover about 6% of the total land area.

The global scale maps and accompanying information presented in this paper are based on a large number of local and regional scale loess studies with variable content and degrees of detail. Small loess areas in Japan (Japanese loam) (Tanino et al., 2015), Northeastern Iran (Muhs, 2013b), Northwestern Turkey (Hou et al., 2015), and Armenia (Wolf et al., 2016) could not be incorporated into the global maps. Due to such omissions and inconsistencies, the presented maps need to be periodically upgraded as more detailed studies on the distribution, particularly in questionable areas, and loess thickness and continuity become available across the globe. In order to speed up this upgrade and to improve the consistency, a coordinated effort at global-scale is needed. The digital nature of the global maps presented in this paper will facilitate these updates, as it allows the geographic base maps to be retrieved at any practical scales needed. For a global representation on a single map, the original source maps were redrawn at their original scales and the original information can be retrieved by zooming into the area of interest. High resolution maps (27,000 × 16,300 pixels, ~ 20 MB) are provided as supplementary materials for this paper, which can be viewed and printed at any practical scale.

Acknowledgements

This study was supported by the following: Key Program of National Natural Science Foundation of China (No. 41630640), Major Program of the National Natural Science Foundation of China (No. 41790445), National Natural Science Foundation of China (No. 41877276), 2014 Fund Program for the Scientific Activities of Selected Returned Overseas Professionals in Shanxi Province, Shanxi Scholarship Council of China, Outstanding Innovative Teams of Higher Learning Institutions of Shanxi, Soft-science Fund Project of Science and Technology in Shanxi, Research Project for Young Sanjin Scholarship of Shanxi, Collaborative Innovation Center for Geohazard Process and Prevention at Taiyuan Univ. of Tech., and Recruitment Program for Young Professionals of China.

Appendix A. Supplementary data

Supplementary data associated with this article can be found, in the online version, at http://dx.doi.org/10.1016/j.earscirev.2019.102947.

References

Ahmad, I., Chandra, R., 2013. Geochemistry of loess-paleosol sediments of Kashmir Valley, India: provenance and weathering. J. Asian Earth Sci. 66, 73–89.

An, Z.S., Wu, G.X., Li, J.P., Sun, Y.B., Liu, Y.M., Zhou, W.J., Cai, Y.J., Duan, A.M., Li, L., Mao, J.Y., Cheng, H., Shi, Z.G., Tan, L.C., Yan, H., Ao, H., Chang, H., Feng, J., 2015. Global monsoon dynamics and climate change. Annu. Rev. Earth Planet. Sci. 43, 29–77.

Antoine, P., Rousseau, D.D., Moine, O., Kunesch, S., Hatté, C., Lang, A., Tissoux, H., Zöller, L., 2009. Rapid and cyclic aeolian deposition during the Last Glacial in European loess: a high-resolution record from Nussloch, Germany. Quat. Sci. Rev. 28, 2955–2973.

Badura, J., Jary, Z., Smalley, I.J., 2013. Sources of loess material for deposits in Poland and parts of Central Europe: the lost Big River. Quat. Int. 296, 15–22.

Ben-Israel, M., Enzel, Y., Amit, R., Erel, Y., 2015. Provenance of the various grain-size fractions in the Negev loess and potential changes in major dust sources to the Eastern Mediterranean. Quat. Res. 83, 105–115.

Bettis III, E.A., Muhs, D.R., Roberts, H.M., Wintle, A.G., 2003. Last glacial loess in the conterminous USA. Quat. Sci. Rev. 22, 1907–1946.

Boenigk, W., Frechen, M., 2001. The loess record in sections at Koblenz–Metternich and Tönchesberg in the middle Rhine Area. Quat. Int. 76/77, 201–209.

Brunotte, E., Maurer, B., Fischer, P., Lomax, J., Sander, H., 2009. A sequence of fluvial and aeolian deposits (desert loess) and palaeosoils covering the last 60 ka in the Opuwo basin (Kaokoland/Kunene Region, Namibia) based on luminescence dating. Quat. Int. 196, 71–85.

Busacca, A., Cremaschi, M., 1998. The role of time versus climate in the formation of deep soils of the Apennine fringe of the Po valley, Italy. Quat. Int. 51/52, 95–107.

Busacca, A.J., Begét, J.E., Markewich, H.W., Muhs, D.R., Lancaster, N., Sweeney, M.R., 2003. Eolian sediments. Develop. Quat. Sci. 1, 275–309.

Butler, B.E., 1956. Parna—an aeolian clay. Aust. J. Sci. 18, 145–151.

Chlachula, J., 2003. The Siberian loess record and its significance for reconstruction of Pleistocene climate change in north-central Asia. Quat. Sci. Rev. 22, 1879–1906.

Coudé-Gaussen, G., 1987. The Perisaharan loess: sedimentological characterization and paleoclimatical significance. Geojournal 15 (2), 177–183.

Coudé-Gaussen, G., 1990. The loess and loess-like deposits along the sides of the western Mediterranean Sea: genetic and palaeoclimatic significance. Quat. Int. 5, 1–8.

Crouvi, O., Amit, R., Enzel, Y., Porat, N., Sandler, A., 2008. Sand dunes as a major proximal dust source for late Pleistocene loess in the Negev Desert, Israel. Quat. Res. 70, 275–282.

Crouvi, O., Amit, R., Enzel, Y., Gillespie, A.R., 2010. Active sand seas and the formation of desert loess. Quat. Sci. Rev. 29, 2087–2098.

Dan, J., 1990. The effect of dust deposition on the soils of the land of Israel. Quat. Int. 5, 107–113.

Dare-Edwards, A.J., 1984. Aeolian clay deposits of south-eastern Australia: parna or loessic clay? Trans. Inst. Br. Geogr. 9 (3), 337–344.

Derbyshire, E., 2001. Geological hazards in loess terrain, with particular reference to the loess regions of China. Earth Sci. Rev. 54, 231–260.

Dodonov, A.E., 2007. Loess records | Central Asia. In: Elias, S.A. (Ed.), Encyclopedia of Quaternary Science. Elsevier Ltd, London, pp. 1418–1429.

Dodonov, A.E., Baiguzina, L.L., 1995. Loess stratigraphy of Central Asia: palaeoclimatic and palaeoenvironmental aspects. Quat. Sci. Rev. 14, 707–720.

Dodonov, A.E., Tchepalyga, A.L., Mihailescu, C.D., Zhou, L.P., Markova, A.K., Trubikhin, V.M., Simakova, A.N., Konikov, E.G., 2000. Last-interglacial records from central Asia to the northern Black Sea shoreline: stratigraphy and correlation. Neth. J. Geosci. 79, 303–311.

Dyke, A.S., Andrews, J.T., Clark, P.U., England, J.H., Miller, G.H., Shaw, J., Veillette, J.J., 2002. The Laurentide and Innuitian ice sheets during the last glacial maximum. Quat. Sci. Rev. 21, 9–31.

Eden, D.N., Hammond, A.P., 2003. Dust accumulation in the New Zealand region since the last glacial maximum. Quat. Sci. Rev. 22, 2037–2052.

Editorial board of Dictionary of Earth Sciences, 2006. Basic sciences volume. Dictionary of Earth Sciences. Geological Publishing House, Beijing (In Chinese).

Eitel, B., Blümel, W.D., Hüser, K., Mauz, B., 2001. Dust and loessic alluvial deposits in Northwestern Namibia (Damaraland, Kaokoveld): sedimentology and palaeoclimatic evidence based on luminescence data. Quat. Int. 76/77, 57–65.

Fitzsimmons, K.E., Marković, S.B., Hambach, U., 2012. Pleistocene environmental dynamics recorded in the loess of the middle and lower Danube basin. Quat. Sci. Rev. 41, 104–118.

Fitzsimmons, K.E., Sprafke, T., Zielhofer, C., Günter, C., Deom, J.M., Sala, R., Iovita, R., 2016. Loess accumulation in the Tian Shan piedmont: implications for palaeoenvironmental change in arid Central Asia. Quat. Int. 1–14. https://doi.org/10.1016/j.quaint.2016.07.041. xxx.

Forno, M.G., 1990. Aeolian and reworked loess in the Turin Hills (northwestern Italy). Quat. Int. 5, 81–87.

Frechen, M., Oches, E.A., Kohfeld, K.E., 2003. Loess in Europe—mass accumulation rates during the last glacial period. Quat. Sci. Rev. 22, 1835–1857.

Fuller, M.L., 1922. Some unusual erosion features in the loess of China. Geogr. Rev. 12, 570–584.

Greene, R.S.B., Cattle, S.R., Mcpherson, A.A., 2009. Role of eolian dust deposits in landscape development and soil degradation in southeastern Australia. Aust. J. Earth Sci. 56, S55–S65.

Grimley, D.A., 2000. Glacial and nonglacial sediment contributions to Wisconsin Episode loess in the central United States. Geol. Soc. Am. Bull. 112 (10), 1475–1495.

Gu, L., Wang, L.Q., Li, M.Z., 2011. Grain sources of the Alashan desert and Loess Plateau in arid and semi-arid regions of northwestern China. J. Arid Land Resour. Environ. 25 (4), 45–49 (In Chinese).

Haase, D., Fink, J., Haase, G., Ruske, R., Pécsi, M., Richter, H., Altermann, M., Jäger, K.D., 2007. Loess in Europe—its spatial distribution based on a European Loess Map, scale 1:2,500,000. Quat. Sci. Rev. 26, 1301–1312.

Haberlah, D., 2007. A call for Australian loess. Area 39 (2), 224–229.

Hesse, P.P., Mctainsh, G.H., 2003. Australian dust deposits: modern processes and the Quaternary record. Quat. Sci. Rev. 22, 2007–2035.
Hill, T.C., 2005. Geochemical Evidence for Weathering in Northwestern European Loess on a Sub-Millennial Scale during the Last Ice Age. PhD Thesis. University of Gloucestershire, Cheltenham.
Hou, S.M., Liu, X.M., Lv, B., Chen, J.S., Wang, T., Zhou, Z.B., Wen, C.H., 2015. Rock magnetic properties of loess in Nallihan, Turkey and its environmental significances. Quat. Sci. 35 (4), 1006–1019 (In Chinese).
Iriondo, M.H., 1997. Models of deposition of loess and loessoids in the upper Quaternary of South America. J. S. Am. Earth Sci. 10 (1), 71–79.
Jefferson, I.F., Evstatiev, D., Karastanev, D., Mavlyanova, N.G., Smalley, I.J., 2003a. Engineering geology of loess and loess-like deposits: a commentary on the Russian literature. Eng. Geol. 68, 333–351.
Jefferson, I.F., Smalley, I.J., Northmore, K., 2003b. Consequences of a modest loess fall over southern and midland England. Mercian Geol. 15 (4), 199–208.
Kang, C.G., Li, C.A., Xie, Y.Y., Chang, Z., Gao, M.X., 2011. Heavy mineral characteristics of eolian loess deposits in Harbin area and its provenance implications. J. Nat. Disasters 20 (4), 43–51 (In Chinese).
Koster, E.A., 1988. Ancient and modern cold-climate aeolian sand deposition: a review. J. Quat. Sci. 3, 69–83.
Kukla, G.J., 1975. Loess stratigraphy of Central Europe. In: Butzer, K.W., Isaac, G.L. (Eds.), After the Australopithecines. Mouton Publishers, Hague, pp. 99–188.
Lebret, P., Lautridou, J.P., 1991. The loess of West Europe. Geojournal 24 (2), 151–156.
Lehmkuhl, F., Zens, J., Krauß, L., Schulte, P., Kels, H., 2016. Loess-paleosol sequences at the northern European loess belt in Germany: distribution, geomorphology and stratigraphy. Quat. Sci. Rev. 153, 11–30.
Lei, X.Y., 2014. The Cause of Formation, Prevention and Cure of Geological Disasters of Loess. Peking University Press, Beijing (In Chinese).
Li, B.C., Sun, J.Z., 2005. Loess and Environment in China. Shaanxi Science and Technology Press, Xi'an (In Chinese).
Liu, T.S., 1965. The Deposition of Loess in China. Science Press, Beijing. (In Chinese.
Liu, T.S., 1985. Loess and the Environment. China Ocean Press, Beijing. (In Chinese.
Liu, D.Y., 2009. Paleo Climate Evolution since the Late Early Pleistocene: An Evidence from a Loess Record, Garze, West Sichuan Plateau. PhD Thesis. Chinese Marine University, Qingdao (In Chinese).
Liu, T.S., An, Z.S., Yuan, B.Y., 1985. Eolian process and dust mantle (loess) in China. Quat. Sci. 6 (1), 113–125 (In Chinese).
Liu, L.J., Li, P.Y., Wang, Y.J., 2000. The grain-size properties and genesis of the loess in Central Shandong Province. Mar. Geol. Quat. Geol. 20 (1), 81–86 (In Chinese).
Liu, T.S., Sun, J.M., Wu, W.X., 2001. Past, present and future of the Chinese loess research: a discussion on the reality of facts and myth. Quat. Sci. 21 (3), 185–207 (In Chinese).
Liu, X.M., Ma, M.M., Wu, H.B., Zhou, Z.B., 2017. Identification of aeolian loess deposits on the Indo-Gangetic Plain (India) and their significance. Sci. China Earth Sci. 60 (3), 428–437.
Luehmann, M.D., Schaetzl, R.J., Miller, B.A., Bigsby, M.E., 2013. Thin, pedoturbated and locally sourced loess in the western Upper Peninsula of Michigan. Aeolian Res. 8, 85–100.
Machalett, B., Frechen, M., Hambach, U., Oches, E.A., Zöller, L., Marković, S.B., 2006. The loess sequence from Remisowka (northern boundary of the Tien Shan Mountains, Kazakhstan)—part I: Luminescence dating. Quat. Int. 152-153, 192–201.
Machalett, B., Oches, E.A., Frechen, M., Zöller, L., Hambach, U., Mavlyanova, N.G., Marković, S.B., Endlicher, W., 2013. Aeolian dust dynamics in Central Asia during the Pleistocene: driven by the long-term migration, seasonality, and permanency of the Asiatic polar front. Geochem. Geophys. Geosyst. 9, 308–313.
Marković, S.B., Smalley, I.J., Hambach, U., Antoine, P., 2009. Loess in the Danube region and surrounding loess provinces: the Marsigli memorial volume. Quat. Int. 198, 5–6.
Marković, S.B., Stevens, T., Kukla, G.J., Hambach, U., Fitzsimmons, K.E., Gibbard, P., Buggle, B., Zech, M., Guo, Z.T., Hao, Q.Z., Wu, H.B., O'Hara Dhand, K., Smalley, I.J., Újvári, G., Sümegi, P., Timar-Gabor, A., Veres, D., Sirocko, F., Vasiljević, D.A., Jary, Z., Svensson, A., Jović, V., Lehmkuhl, F., Kovács, J., Svirčev, Z., 2015. Danube loess stratigraphy - Towards a pan-European loess stratigraphic model. Earth-Sci. Revs. 148, 228–258.
Marković, S.B., Fitzsimmons, K.E., Sprafke, T., Gavrilović, D., Smalley, I.J., Jović, V., Svirčev, Z., Gavrilov, M.B., Bešlin, M., 2016. The history of Danube loess research. Quat. Int. 399, 86–99.
Mason, J.A., Nater, E.A., Zanner, C.W., Bell, J.C., 1999. A new model of topographic effects on the distribution of loess. Geomorphology 28, 223–236.
Muhs, D.R., 2007. Loess deposits, origins and properties. In: Elias, S.A. (Ed.), Encyclopedia of Quaternary Science. Elsevier, London, pp. 1405–1418.
Muhs, D.R., 2013a. The geologic records of dust in the Quaternary. Aeolian Res. 9, 3–48.
Muhs, D.R., 2013b. Loess and its geomorphic, stratigraphic, and paleoclimatic significance in the Quaternary. In: In: Shroder, J., Lancaster, N., Sherman, D.J., Baas, A.C.W. (Eds.), Treatise on Geomorphology 11. Aeolian Geomorphology. Academic Press, San Diego, pp. 149–183.
Muhs, D.R., Bettis III, E.A., 2000. Geochemical variations in Peoria loess of western Iowa indicate paleowinds of midcontinental North America during last glaciation. Quat. Res. 53, 49–61.
Muhs, D.R., Bettis III, E.A., 2003. Quaternary loess-paleosol sequences as examples of climate-driven sedimentary extremes. In: Chan, M.A., Archer, A.W. (Eds.), Extreme Depositional Environments: Mega End Members in Geologic Time. Geological Society of America, Boulder, pp. 53–74 Special Paper 370.
Muhs, D.R., Ager, T.A., Bettis III, E.A., Mcgeehin, J., Been, J.M., Begét, J.E., Pavich, M.J., Stafford Jr., T.W., Stevens, D.A.S.P., 2003. Stratigraphy and palaeoclimatic significance of Late Quaternary loess-palaeosol sequences of the Last Interglacial-Glacial cycle in central Alaska. Quat. Sci. Rev. 22 (18), 1947–1986.
Muhs, D.R., Cattle, S.R., Crouvi, O., Rousseau, D.D., Sun, J.M., Zárate, M.A., 2014. Loess records. In: Knippertz, P., Stuut, J.W. (Eds.), Mineral Dust: A Key Player in the Earth System. Springer Verlag, Berlin, pp. 411–441.
Muhs, D.R., Pigati, J.S., Budahn, J.R., Skipp, G.L., Bettis III, E.A., Jensen, B., 2018. Origin of last-glacial loess in the western Yukon-Tanana Upland, central Alaska, USA. Quat. Res. 89, 797–819.
Murton, J.B., Goslar, T., Edwards, M.E., Bateman, M.D., Danilov, P.P., Savvinov, G.N., Gubin, S.V., Ghaleb, B., Haile, J., Kanevskiy, M., Lozhkin, A.V., Lupachev, A.V., Murton, D.K., Shur, Y., Tikhonov, A., Vasil'chuk, A.C., Vasil'chuk, Y.K., Wolfe, S.A., 2015. Palaeoenvironmental interpretation of yedoma silt (ice complex) deposition as cold-climate loess, Duvanny Yar, northeast Siberia. Permafr. Periglac. Process. 26, 208–288.
National Research Council Committee for the Study of Eolian Deposits Division of Geology and Geography (U.S.), 1952. Pleistocene Eolian Deposits of the United States, Alaska, and Parts of Canada, 1:2,500,000. Geological Society of America, Boulder.
Nettleton, W.D., Chadwick, O.A., 1996. Late Quaternary, redeposited loess-soil developmental sequences, South Yemen. Geoderma 70, 21–36.
Nie, J.S., Stevens, T., Rittner, M., Stockli, D., Garzanti, E., Limonta, M., Bird, A., Andò, S., Vermeesch, P., Saylor, J., Lu, H.Y., Breecker, D., Hu, X.F., Liu, S.P., Resentini, A., Vezzoli, G., Peng, W.B., Carter, A., Ji, S.C., Pan, B.T., 2015. Loess Plateau storage of Northeastern Tibetan Plateau-derived Yellow River sediment. Nat. Commun. 6, 8511.
Obruchev, V.A., 1911. The question of the origin of loess—in defense of the aeolian hypothesis. Izv. Tomsk. Tekhnol. Inst. 33.
Obruchev, V.A., 1933. The problem of loess. The Transactions of the 2-nd International Congress of Association on Quaternary Research 2, 115–137.
Obruchev, V.A., 1958. Sand and loess issues. Science Press, Beijing (In Chinese).
Pant, R.K., 1993. Spread of loess and march of desert in western India. Curr. Sci. 64 (11 − 12), 841–847.
Pécsi, M., 1968. Loess. In: Fairbridge, R.W. (Ed.), Geomorphology. Encyclopedia of Earth Science. Springer, Berlin, Heidelberg, pp. 674–678.
Pécsi, M., 1990. Loess is not just the accumulation of dust. Quat. Int. 7/8, 1–21.
Peng, S.Z., Gao, Z.D., Wu, X.P., Zhang, L.B., Liang, M.Y., Qiao, Y.S., 2007. Grain-size distribution and genesis of loess in the Qingzhou area, Shandong. J. Geom. 13 (4), 315–321 (In Chinese).
Péwé, T.L., 1975. Quaternary Geology of Alaska. United States Government Printing Office, Washington.
Péwé, T.L., Journaux, A., 1983. Origin and Character of Loesslike Silt in Unglaciated South-Central Yakutia, Siberia, U.S.S.R. United States Government Printing Office, Washington.
Porter, S.C., 2007. Loess records | China. In: Elias, S.A. (Ed.), Encyclopedia of Quaternary Science. Elsevier, London, pp. 1429–1440.
Price, A.B., Nettleton, W.D., Bowman, G.A., Clay, V.L., 1988. Selected properties, distribution, source, and age of eolian deposits and soils of southwest Colorado. Soil Sci. Soc. Am. J. 52, 450–455.
Prins, M.A., Zheng, H.B., Beets, K., Troelstra, S., Bacon, P., Kamerling, I., Wester, W., Konert, M., Huang, X.T., Ke, W., Vandenberghe, J., 2009. Dust supply from river floodplains: the case of the lower Huang He (Yellow River) recorded in a loess–palaeosol sequence from the Mangshan Plateau. J. Quat. Sci. 24, 75–84.
Pye, K., 1987. Loess. Aeolian Dust and Dust Deposits. Academic Press, London.
Pye, K., 1995. The nature, origin and accumulation of loess. Quat. Sci. Rev. 14, 653–667.
Ren, M.E., 2006. Sediment discharge of the Yellow River, China: past, present and future—a synthesis. Adv. Earth Science 21 (6), 551–563.
Renssen, H., Kasse, C., Vandenberghe, J., Lorenz, S.J., 2007. Weichselian late Pleniglacial surface winds over northwest and central Europe: a model–data comparison. J. Quat. Sci. 22, 281–293.
Richthofen, F., 1877. China: Ergebnisse Eigener Reisen und Darauf Gegründeter Studien. Verlag von Dietrich Reimer, Berlin.
Roberts, H.M., Muhs, D.R., Bettis III, E.A., 2007. Loess records | North America. In: Elias, S.A. (Ed.), Encyclopedia of Quaternary Science. Elsevier, London, pp. 1456–1466.
Rousseau, D.-D., Derbyshire, E., Antoine, P., Hatté, C., 2007. Loess records | Europe. In: Elias, S.A. (Ed.), Encyclopedia of Quaternary Science. Elsevier, London, pp. 1440–1456.
Sayago, J.M., Collantes, M.M., Karlson, A., Sanabria, J., 2001. Genesis and distribution of the late Pleistocene and Holocene loess of Argentina: a regional approximation. Quat. Int. 76, 247–257.
Schaetzl, R.J., Loope, W.L., 2008. Evidence for an eolian origin for the silt enriched soil mantles on the glaciated uplands of eastern Upper Michigan, USA. Geomorphology 100, 285–295.
Schaetzl, R.J., Larson, P.H., Faulkner, D.J., Running, G.L., Jol, H.M., Rittenour, T.M., 2018a. Eolian sand and loess deposits indicate west-northwest paleowinds during the late Pleistocene in western Wisconsin, USA. Quat. Res. 89, 769–785.
Schaetzl, R.J., Bettis III, E.A., Crouvi, O., Fitzsimmons, K.E., Grimley, D.A., Hambach, U., Lehmkuhl, F., Marković, S.B., Mason, J.A., Owczarek, P., Roberts, H.M., Rousseau, D.-D., Stevens, T., Vandenberghe, J., Zárate, M., Veres, D., Yang, S.L., Zech, M., Conroy, J.L., Dave, A.K., Faust, D., Hao, Q.Z., Obreht, I., Prud'homme, C., Smalley, I., Tripaldi, A., Zeeden, C., Zech, R., 2018b. Approaches and challenges to the study of loess—Introduction to the LoessFest special issue. Quat. Res. 89, 563–618.
Schirrmeister, L., Strauss, J., Wetterich, S., Grosse, G., Overduin, P.P., 2013. Quality and distribution of frozen organic matter (old, deep, fossil carbon) in Siberian permafrost. Geophys. Res. Abstr. 15.
Smalley, I.J., 1966. The properties of glacial loess and the formation of loess deposits. J. Sediment. Petrol. 36, 669–676.
Smalley, I.J., 1978. The New Zealand loess and the major categories of loess classification. Search 9, 281–282.
Smalley, I.J., 1995. Making the material: the formation of silt sized primary mineral

particles for loess deposits. Quat. Sci. Rev. 14, 645–651.
Smalley, I.J., 2008. A call for Australian loess: discussion and commentary. Area 40, 131–134.
Smalley, I.J., Derbyshire, E., 1990. The definition of 'ice-sheet' and 'mountain' loess. Area 22, 300–301.
Smalley, I.J., Krinsley, D.H., 1978. Loess deposits associated with deserts. Catena 5, 53–66.
Smalley, I.J., Leach, J.A., 1978. The origin and distribution of the loess in the Danube basin and associated regions of east-central Europe—a review. Sediment. Geol. 21, 1–26.
Smalley, I.J., Vita-Finzi, C., 1968. The formation of fine particles in sandy deserts and the nature of 'desert' loess. J. Sediment. Petrol. 38, 766–774.
Smalley, I.J., Jefferson, I.F., Dijkstra, T.A., Derbyshire, E., 2001. Some major events in the development of the scientific study of loess. Earth Sci. Rev. 54, 5–18.
Smalley, I.J., Mavlyanova, N.G., Rakhmatullaev, K.L., Shermatov, M.S., Machalett, B., Dhand, K.O., Jefferson, I.F., 2006. The formation of loess deposits in the Tashkent region and parts of Central Asia; and problems with irrigation, hydrocollapse and soil erosion. Quat. Int. 152-153, 59–69.
Smalley, I.J., O'Hara-Dhand, K., Wint, J., Machalett, B., Jary, Z., Jefferson, I.F., 2009. Rivers and loess: the significance of long river transportation in the complex event-sequence approach to loess deposit formation. Quat. Int. 198, 7–18.
Smalley, I., Marković, S.B., Svirčev, Z., 2011. Loess is [almost totally formed by] the accumulation of dust. Quat. Int. 240, 4–11.
Smalley, I.J., O'Hara-Dhand, K., Kwong, J., 2014. China: materials for a loess landscape. Catena 117, 100–107.
Smith, B.J., Wright, J.S., Whalley, W.B., 2002. Sources of non-glacial, loess-size quartz silt and the origins of "desert loess". Earth Sci. Rev. 59, 1–26.
Solarska, A., Hose, T.A., Vasiljević, D.A., Mroczek, P., Jary, Z., Marković, S.B., Widawski, K., 2013. Geodiversity of the loess regions in Poland: inventory, geoconservation issues, and geotourism potential. Quat. Int. 296, 68–81.
Sprafke, T., Obreht, I., 2016. Loess: rock, sediment or soil—what is missing for its definition? Quat. Int. 399, 198–207.
Stevens, T., Carter, A., Watson, T.P., Vermeesch, P., Andò, S., Bird, A.F., Lu, H., Garzanti, E., Cottam, M.A., Sevastjanova, I., 2013. Genetic linkage between the Yellow River, the Mu Us desert and the Chinese Loess Plateau. Quat. Sci. Rev. 78, 355–368.
Sun, J.M., 2002a. Provenance of loess material and formation of loess deposits on the Chinese Loess Plateau. Earth Planet. Sci. Lett. 203, 845–859.
Sun, J.M., 2002b. Source regions and formation of the loess sediments on the high mountain regions of northwestern China. Quat. Res. 58, 341–351.
Sun, J.Z., 2005. Loessology. Hong Kong Archaeological Society, Hong Kong (In Chinese).
Svendsen, J.I., Alexanderson, H., Astakhov, V.I., Demidov, I., Dowdeswell, J.A., Funder, S., Gataullin, V., Henriksen, M., Hjort, C., Houmark-Nielsen, M., Hubberten, H.W., Ingólfsson, O., Jakobsson, M., Kjær, K.H., Larsen, E., Lokrantz, H., Lunkka, J.P., Lysa, A., Mangerud, J., Matiouchkov, A., Murray, A., Möller, P., Niessen, F., Nikolskaya, O., Polyak, L., Saarnisto, M., Siegert, C., Siegert, M.J., Spielhagen, R.F., Stein, R., 2004. Late Quaternary ice sheet history of northern Eurasia. Quat. Sci. Rev. 23, 1229–1271.
Tanino, K., Hosono, M., Watanabe, M., 2015. Distribution and formation of tephric-loess dunes in northern and eastern Japan. Quat. Int. 397, 234–249.
Tutkovskii, P.A., 1899. The question of the method of loess formation. Zemlevedenie 213–311.
Ulrich, R., 1950. Some chemical changes accompanying profile formation of nearly level soils developed from Peorian loess in southwestern Iowa. Soil Sci. Soc. Proc. 15, 324–329.
Vandenberghe, J., 2013. Grain size of fine-grained windblown sediment: a powerful proxy for process identification. Earth Sci. Rev. 121, 18–30.
Virlet D'Aoust, P.T., 1857. Observations sur un terrain d'origine météorique ou de transport aérien qui existe au Mexique, et sur le phénomène des trombes de poussière auquel il doit principalement son origine. Bull. Geol. Soc. France 15, 129–139.
Wang, T., 1990. Formation and evolution of Badain Jirin sandy desert, China. J. Desert Res. 10 (1) (29-40. (In Chinese).
Wang, Y.Y., Zhang, Z.H., 1980. Loess in China. Shaanxi people's Art Publishing House, Xi'an (In Chinese).
Wang, Y.N., Peng, S.Z., Feng, Z., Zhang, W., Ding, M., 2014. Grain-size characteristics of loess deposits and it's implication in the northern piedmont of the central Shandong Mountainous region. J. Arid Land Resour. Environ. 28 (8), 156–160 (In Chinese).
Williams, M., 2015. Interactions between fluvial and eolian geomorphic systems and processes: examples from the Sahara and Australia. Catena 134, 4–13.
Wolf, D., Baumgart, P., Meszner, S., Fülling, A., Haubold, F., Sahakyan, L., Meliksetian, K., Faust, D., 2016. Loess in Armenia – stratigraphic findings and palaeoenvironmental indications. Proc. Geol. Assoc. 127, 29–39.
Wright, J.S., 2001. "Desert" loess versus "glacial" loess: quartz silt formation, source areas and sediment pathways in the formation of loess deposits. Geomorphology 36, 231–256.
Xia, Z.K., Bruce, J.G., Crozier, M.J., 1993. Comparative study of New Zealand loess with China loess. Acta Geograph. Sin. 48 (4), 337–347 (In Chinese).
Yang, X.Y., Liu, T.S., 2008. Eurasian loess belt and ancient human activities during the early Paleolithic age. Quat. Sci. 28 (6), 978–987 (In Chinese).
Yang, Q.Y., Zhang, B.P., Zheng, D., 1988. On the boundary of the Loess Plateau. J. Nat. Resour. 3 (1), 9–15 (In Chinese).
Yin, Z.Q., Qin, X.G., 2010. The Yushu loess deposition in eastern Songnen Basin since the last glacial period and its environmental significance. Geol. China 37 (1), 212–222 (In Chinese).
Zárate, M.A., 2003. Loess of southern South America. Quat. Sci. Rev. 22, 1987–2006.
Zárate, M.A., 2007. Loess records | South America. In: Elias, S.A. (Ed.), Encyclopedia of Quaternary Science. Elsevier, London, pp. 1466–1479.
Zhang, Z.H., 1983. The compilation principle of landscape type map of Chinese Loess Plateau. Hydrogeol. Eng. Geol. 2, 29–33 (In Chinese).
Zhang, Z.H., 2000. Nine Greet Bends with Miles of Sands in Yellow River—Yellow River and Loess Plateau. Tsinghua University Press, Beijing and JiNan University Press, Guangzhou (In Chinese).
Zheng, L., 2018. Provenances of the major loess deposits in eastern China based on Sr and Nd isotopic characteristics. Geol. J. China Univ. 24 (2), 246–250 (In Chinese).
Zhou, M., 2011. Practical Atlas of the World. Sinomaps Press, Beijing. (In Chinese.
Zhu, S.G., Sang, G.S., Zhu, L.T., 2009. Western Landmarks: Loess Plateau. Shanghai Scientific and Technological Literature Press, Shanghai (In Chinese).